2006

Verification of the whitetopping thickness design procedure for asphalt concrete overlaid Portland cement concrete pavements

Toni Raenette Tabbert
Iowa State University

Verification of the whitetopping thickness design procedure for asphalt concrete overlaid Portland cement concrete pavements

by

Toni Raenette Tabbert

A thesis submitted to the graduate faculty
in partial fulfillment of the requirements for the degree of
MASTER OF SCIENCE

Major: Civil Engineering (Geotechnical and Structural Engineering)

Program of Study Committee:

James K. Cable, Co-major Professor
Halil Ceylan, Co-major Professor
Fouad S. Fanous, Co-major Professor
Loren Zachary

Iowa State University
Ames, Iowa
2006

UMI Number: 1439900

ProQuest Information and Learning Company
300 North Zeeb Road
P.O. Box 1346
Ann Arbor, MI 48106-1346

TABLE OF CONTENTS

LIST OF FIGURES iv

LIST OF TABLES v

1.0 INTRODUCTION 1
1.1 Project Background 1
1.2 Objectives 3
1.3 Research Approach 3

2.0 LITERATURE REVIEW 5
2.1 Fundamental Behavior of Whitetopping Pavements 5
2.2 Pavement Whitetopping Studies 6
2.2.1 Other Pavement Design Methodologies 7
2.3 Evaluation of an Existing AC/PCC Pavement 7
2.3.1 Data Collection 7
2.4 Development of Ioannides "Equivalent" Plate Method 8
2.5 Finite Element Modeling Techniques for Composite Pavements 10
2.5.1 Modeling of Concrete and Asphalt Layers 11
2.5.2 Foundation Modeling Techniques 11

3.0 MODELING OF IOWA HIGHWAY 13 13
3.1 Modeling of Composite Pavement for Finite Element Analysis 13
3.1.1 Types of Element Used to Model Iowa Highway 13 14
3.1.1.1 Plate Elements 14
3.1.1.2 Solid Elements 14
3.2 Finite Element Modeling of the "Equivalent" Plate 15
3.3 Finite Element Modeling of the Composite System (Iowa Highway 13) 15

4.0 FIELD EVALUATION OF IOWA HIGHWAY 13 17
4.1 Visual Survey 17
4.2 Nondestructive Deflection Testing 17
4.3 Soil Classification 18
4.3.1 Soil Survey Summary 19
4.3.2 Visual Soil Classification Survey 21

5.0 DATA ANALYSIS 22
5.1 Determination of Properties for AC/PCC and PCC/AC/PCC Pavements 22
5.1.2 AC Elastic Modulus 22
5.1.3 Effects of temperature on the AC elastic modulus 23
5.1.4 Corrections for Determining the In Situ AC Elastic Modulus 24
5.1.5 Deflection of the Existing PCC Slab 24
5.1.6 Deflection Basin of the PCC ($AREA_{PCC}$) 25
5.1.7 Slab Size Correction 26

5.1.8 Dynamic Modulus of Subgrade Reaction 27
5.1.8.1 Relationship between a liquid and solid foundation 27
5.1.9 Existing PCC Elastic Modulus 29
5.2 Determination of Stresses using Ioannides "Equivalent" Plate Method 31
5.2.1 Evaluation of the "Equivalent" Plate for an Unbonded AC/PCC Pavement 31
5.2.2 Evaluation of the "Equivalent" Plate for a Bonded AC/PCC Pavement 32
5.3 Comparison of ANSYS and ISLAB2000 with Ioannides "Equivalent" Plate Method 34
5.3.1 Evaluation of Westergaard's Equations for an Unbonded AC/PCC Pavement 34
5.3.2 Application of the "Equivalent" Plate Method to an AC/PCC Pavement 35
5.3.3 Application of the "Equivalent" Plate Method to a PCC/AC/PCC Pavement 39

6.0 SUMMARY, CONCLUSION, AND RECOMMENDATIONS 42
6.1 Summary 42
6.2 Conclusions 43
6.3 Future Research Recommendations 43

APPENDIX A 45

APPENDIX B 48

APPENDIX C 61

APPENDIX D 67

APPENDIX E 72

APPENDIX F 77

REFERENCES 82

LIST OF FIGURES

Figure 1-1 Cross-Section of Iowa Highway 13 2
Figure 2-1 TWT and UTW Behavior under Flexural Loading [6] 5
Figure 2-2 Typical Deflection Basin [13] 8
Figure 2-3 Liquid Foundation under a Plate Element 12
Figure 3-1 Modeling of the Pavement and Soil using Solid Elements 16
Figure 4-1 Schematic of FWD Deflection Sensors 18
Figure 4-2 Iowa Highway 13 Soil Associations 19
Figure 5-1 Deflection of the Unbonded AC/PCC Pavement 36
Figure 5-2 Summary of Stress Distributions in the Unbonded AC/PCC Pavement 37
Figure 5-3 Summary of Stress Distributions in the Bonded AC/PCC Pavement 38
Figure 5-4 Summary of Stress Distributions in the Unbonded PCC/AC/PCC Pavement 40
Figure 5-5 Summary of Stress Distributions in the Bonded PCC/AC/PCC Pavement 41

LIST OF TABLES

Table 5-1 Elastic Modulus of the Soil Summary 29
Table 5-2 Summary of Material Properties 31
Table 5-3 Summary of the "Equivalent" Plate Verification 35
Table 5-4 Summary of Displacements in the Unbonded AC/PCC Pavement 36
Table 5-5 Summary of Displacements in the Bonded AC/PCC Pavement 38
Table 5-6 Summary of Displacements in the Unbonded PCC/AC/PCC Pavement 39
Table 5-7 Summary of Displacements in the Bonded PCC/AC/PCC Pavement 40

1.0 INTRODUCTION

Iowa is one of few states with a large number of Portland Cement Concrete (PCC) pavements. Many of these pavements were designed with an initial design life of 20 years. By the 1970's these pavement systems had either reached or exceeded their design life. In order to rehabilitate these old pavements multiple layers of Asphalt Concrete (AC) were placed over the existing PCC slabs which increased the life of the roadway for about 10 to 15 years [1]. However, there was a need for an alternative with a longer life and lower life-cycle cost. With improvements in paving technology such as the slipform paver and the ability to obtain high early age strength, PCC overlays soon became that alternative.

Since PCC overlays are a fairly new concept to the paving industry, their design and construction has been based on empirical methods. Recent research has provided engineers with more mechanistic design possibilities. Before these mechanistic design procedures can be applied to existing AC overlaid PCC (AC/PCC) pavements, engineers need a practical means to determine the properties of the composite pavement. Also, many of the current overlay design procedures were developed for an existing single placed layer of pavement and are not applicable to the two layered AC/PCC pavements. In the *TR 511* [2] report, a method was developed so that the single placed layer concept could be applied to the analysis and design of overlays for AC/PCC pavements.

1.1 Project Background

In 1994, an Ultra Thin Whitetopping (UTW) was placed on a 7.2 mile segment of Iowa Highway 21, near Belle Plain, Iowa. When the highway was constructed, it was the largest UTW in the United States. This research focused on the condition of the bond at the interface between the PCC overlay and the existing AC pavement overtime, with consideration given to a combination of various factors. These factors include varying the depth of the overlay, joint spacing, surface preparation, incorporation of various types of fiber reinforcement, and joint preparation/sealing [3].

In 2002, the Iowa Department of Transportation (IDOT) initiated a second project to examine and verify the findings of the Iowa Highway 21 research. The project is a 9.6 mile long segment located north of Manchester, Iowa along Iowa Highway 13. This highway was originally built in 1931 and constructed as an 18 ft wide, thickened edge PCC pavement with a 7" depth at the center line and a 10" depth along the outer edge. In 1964, the PCC driving surface was rehabilitated with a 2" AC overlay. In 1984, it was overlaid again with an additional 3" of AC and widened from 18 ft to 24 ft. In 2002, Iowa Highway 13 was rehabilitated with either a 3.5" or a 4.5" PCC overlay. When the highway was overlaid in 2002 it was still in good structural condition, but cracking and deterioration of the AC overlay was extensive. In addition to the overlay, a 5 ft widening unit was placed on each side of the roadway extending the driving surface to 28 ft wide [1]. The proposed cross section of the road way is shown in Figure 1-1.

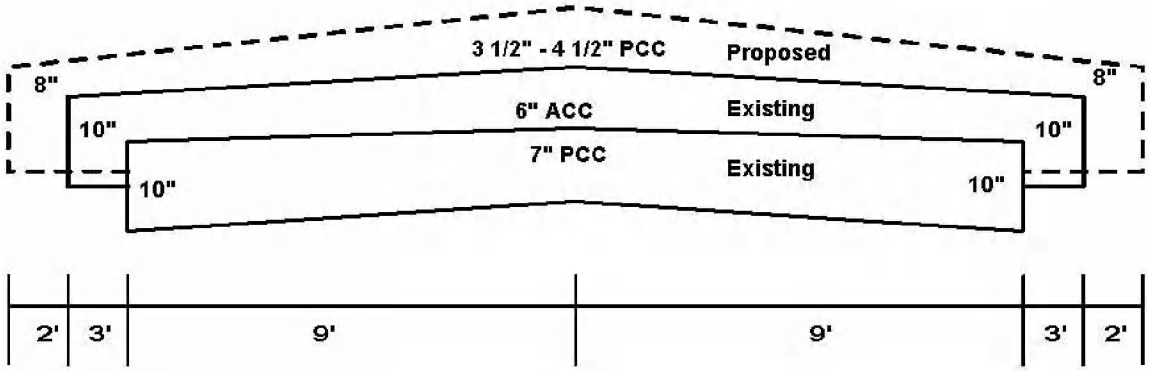

Figure 1-1 Cross-Section of Iowa Highway 13

The Iowa Highway 21 project identified outer boundaries for each of the variables (panel size of 2', 4', 6', and 12' squares, depth of overlay 2", 4", 6", and 8") in terms of performance. Panel sizes of 4.5', 6', and 9' squares and overlay depths of 3.5" and 4.5" were used to further delineate the relationships in the Iowa Highway 13 project. Data collected on deflections and performance (visual distress) from the Iowa Highway 13 project is utilized for the analysis and verification of design concepts discussed in this research.

The study presented here is an extension of previous research. Its purpose was to investigate and verify existing methodologies related to analysis and design of PCC overlays. It also presents modifications that may be used in future research.

1.2 Objectives

The primary objective of this research was to review a previously developed PCC overlay design procedure and apply plate theory to analyze displacements and overlay material stresses. In order to achieve this objective, the following sub-objectives were also considered:

- Apply the backcalculation procedure developed by Hall and Darter [4] to determine the pavement properties of an existing AC/PCC pavement and the modulus of subgrade reaction of it's foundation
- Develop multiple finite element models to verify the procedure for an "equivalent" plate based on two layered AC/PCC pavements outlined in *Structural Evaluation of Base Layers in Concrete Pavement Systems* [5]
- Develop an analytical model to verify deflection and stress calculations for a two layered AC/PCC pavement based on Ioannides [5] "equivalent" plate method
- Modify/revise the previously developed methodology for application to an existing PCC overlaid AC/PCC pavement system
- Develop an analytical finite element model to investigate the application of modified calculations to three layered pavement systems

1.3 Research Approach

To obtain the objectives mentioned above, the following tasks were performed:

- Study field performance of Iowa Highway 13 considering on the following conditions:
    - Distress of the roadway

  - Structural condition of the roadway
  - Evaluation of the soil and drainage conditions
- Collection of data regarding the structural condition of the pavement using a Falling Weight Deflectometer (FWD) prior to overlay
- Collection of field data for the determination of soil properties
- Determination of information regarding properties of the roadway and its consecutive layers.
- Calculation of an "equivalent" thickness for the composite pavement before and after overlay placement
- Determination of deflections and stresses in single layer and multi-layered pavement systems using Ioannides "equivalent" plate method [5]
- Comparison of the calculated results with values obtained from Finite element models

2.0 LITERATURE REVIEW

2.1 Fundamental Behavior of Whitetopping Pavements

The behavior of Thin Whitetopping (TWT) and UTW pavements is uniquely different from those of conventional PCC and HMA pavements. TWT and UTW are designed and constructed with the assumption that the whitetopping is fully bonded to the existing pavement, resulting in a composite structure [7]. The condition of the bond at the interface significantly affects how traffic and environmental loads are carried.

How stresses are distributed in a bonded system verses an unbonded system is illustrated in Figure 2-1. The composite action of the bonded system causes stresses in the top PCC layer to be considerably lower when compared to the unbonded case. Therefore, thinner whitetoppings can be designed for fully bonded pavement systems [8].

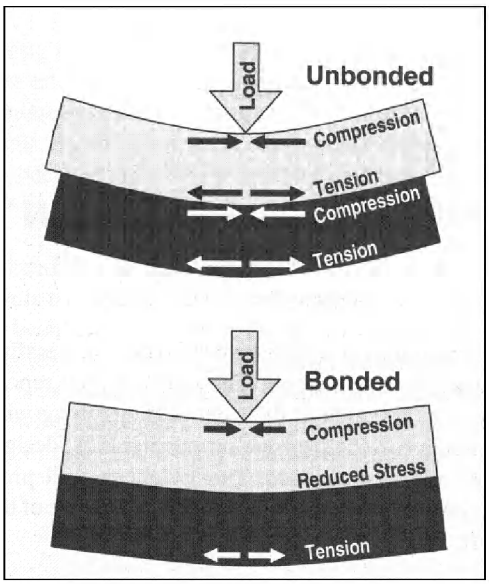

Figure 2-1 TWT and UTW Behavior under Flexural Loading [6]

This type of stress distribution is also applicable to AC/PCC and PCC overlaid on to AC/PCC (PCC/AC/PCC) pavements. However, during construction only a partial bond is

normally achieved. As a result the actual stresses occurring in a composite pavement will lie somewhere between the bonded and unbonded cases.

2.2 Pavement Whitetopping Studies

In the 1900's, the Portland Cement Association (PCA) began a study to develop mechanistic UTW pavement design guidelines. As part of this experiment, researchers studied the theoretical behavior of UTW pavements, performed field load testing, and developed a 3-dimensional (3-D) model of the PCC overlaid AC roadway. The parametric study using the 3-D model considered pavement characteristics such as load position, alignment of cracks in the existing AC with the edges of the new PCC slab, load transfer, and bond condition between the PCC slab and AC pavement. Stresses were evaluated within three locations of the pavement system; at the surface of the PCC slab, at the bottom of the PCC slab (i.e. at the interface), and at the bottom of the AC layer. The PCA study showed the bond condition significantly affected the degree of stress experienced by the pavement when subjected to load. It was also shown that stresses were affected by the condition of the existing AC. Results from the analytical study were confirmed with field instrumentation and load testing which lead to a reasonable design procedure for UTW's [9].

As part of the PCA study, the Colorado DOT (CDOT) constructed two whitetopping projects. Using the findings from these pavements the CDOT implemented a second project in 2001. Similar to the PCA study the CDOT experimental pavements were instrumented and load tested. However, these pavements were located in areas with a higher traffic volume. As a result a thicker whitetopping was constructed. Unlike the design guidelines that resulted from the 1998 project, the revised design procedure took into consideration the effects of slab thickness and joint spacing [10].

2.2.1 Other Pavement Design Methodologies

The following methodologies were described in report *TR-511* [2].

- Transtec Overlay Design [11]
- Illinois (Riley et al. 2005) [12]

The details of these methodologies are not described here due to the nature of the objectives for this thesis, shown above.

2.3 Evaluation of an Existing AC/PCC Pavement

AC overlaid concrete pavements are one of the most difficult types of pavements to evaluate structurally. This is due to the complex behavior of the composite structure and the lack of knowledge of how to interpret the structural analysis results. In recent research Hall and Darter developed a structural evaluation method that could be applied to AC/PCC pavements. This procedure uses deflection data measured on an AC/PCC pavement to backcalculate the elastic moduli of the PCC slab and its foundation. Hall and Darter also state that backcalculation results can be used to identify the amount of deterioration present in the existing PCC slab [4].

2.3.1 Data Collection

Before the type of rehabilitation method is selected, evaluations considering a pavements function, structural condition, drainage, and condition of the AC material are performed. Assessment of the pavement is done in the form of distress surveys, nondestructive deflection testing (NDT), and materials sampling and testing. Of the three methods, distress surveys are the most useful to engineers [4].

Nondestructive deflection testing is done with the use of a Falling Weight Deflectometer (FWD). For the backcalculation method described in this paper, a target load of 9000 pounds is used and deflection measurements are taken from sensors located at the center of the load plate (d_0) and at 12 (d_{12}), 24 (d_{24}), and 36 (d_{36}), inches from the center of the load plate [4]. Deflections taken from these locations are then used to calculate the area of the deflection basin. A representation of the deflection basin and how it relates to FWD loading can be seen in Figure2-2.

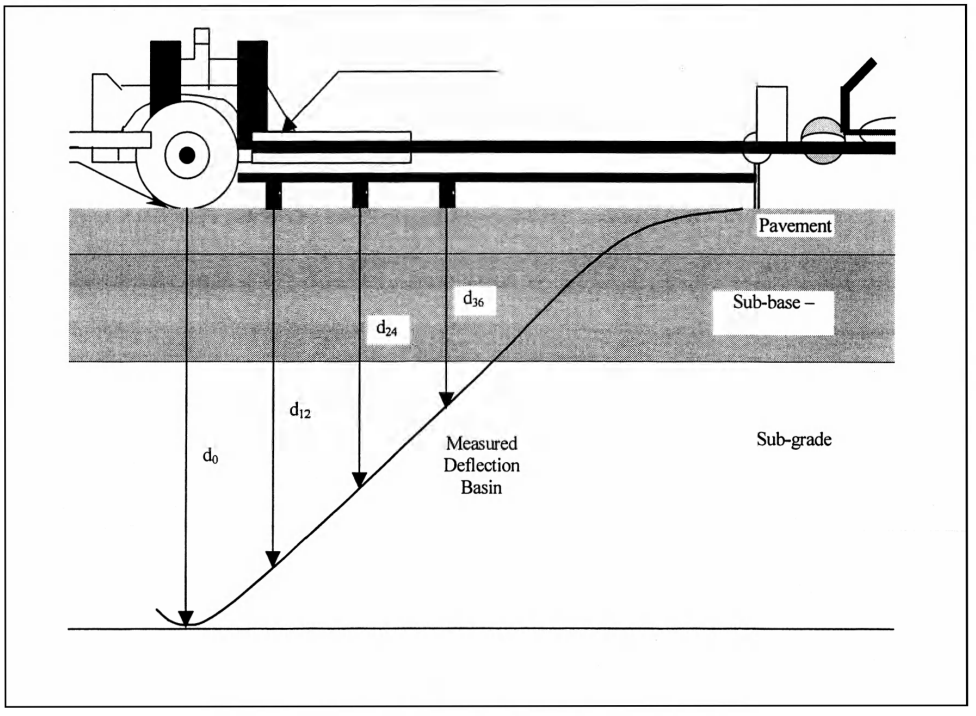

Figure 2-2 Typical Deflection Basin [13]

2.4 Development of Ioannides "Equivalent" Plate Method

Closed form analytical solutions have been used for PCC pavement design and analysis for the past 75 years. The same restrictive assumptions that led to Westergaard's equations also govern the development of mechanistic-based design procedures in use today. These assumptions are listed below;

- Slab size has no effect on the pavement system
- The pavement system is only a single slab panel, therefore it experiences no load transfer
- The pavement system is constructed as a single-placed layer (SPL) with no base or subbase
- The pavement system rests an a foundation with no rigid bottom (semi-infinite foundation)
- The pavement system experiences a single tire print and multiple wheel loads are not considered
- The pavement system experiences no temperature or moisture effect (no curling and warping)

In concrete pavement construction, the actual behavior of the pavement system disobeys all of these assumptions. Therefore many analytical solutions must be adjusted before a reasonable design can be developed. In PCC pavement design it is common to consider feasible alternatives such as the use of AC. The single placed layer assumption does not allow for this alternative because AC pavement construction utilizes either a base or sub-base, creating a multi-layered pavement system [5].

In an effort to accommodate multi-layered pavements, an analysis and design procedure based on layered elastic theory was considered [14]. Although the layered elastic theory proved to be useful, it was unable to account for the occurrence of curling and warping experienced by a pavement slab during temperature changes. Originally, the design of single placed layer systems accommodated for this phenomenon by utilizing plate theory based designs. It was suggested by Odemark in the development of his "equivalent thicknesses method" that the layered elastic theory could be used as an extension of plate theory based designs [15].

This led to the development of an analysis procedure that incorporates the use of an "equivalent" plate to determine maximum responses experienced by multi-layered pavements. The proposed procedure starts by considering two placed layers and their

foundation, as a composite plate resting on an elastic foundation (liquid or solid). It then proposes that there exists an imaginary SPL or plate of homogeneous material resting on the same elastic foundation. This SPL is also known as the "equivalent" plate. It is assumed that the "equivalent" plate is a representation of the composite plate. Therefore, material properties, deformation, and moment carried by both systems are assumed to be equal [5].

In order to develop an analytical process that uses the "equivalent" plate to determine maximum responses in a composite pavement system the following assumptions must be made:

- The development of the "equivalent" plate is based on medium thick plate theory [16]
- The "equivalent" plate is of uniform cross section and experiences elastic bending
- The layers of the composite plate do not separate in the vertical direction during bending
- Deformation of the "equivalent" plate mimics the deformation of the composite plate
- Poisson's ratio is equal to a single value in both the composite plate and the "equivalent" plate
- The total moment acting on the composite plate is equal to the moment acting on the "equivalent" plate
- The total flexural stiffness of the composite plate is equal to that of the "equivalent" plate
- The material properties of the "equivalent" plate are represented by the material properties of the composite plate

A more detailed description of the analytical process can be found in the paper *Structural Evaluation of Base Layers in Concrete Pavement Systems* [5]

2.5 Finite Element Modeling Techniques for Composite Pavements

Finite element programs based on traditional theories of analyzing thin plates on Winkler foundations such as ISLAB2000, J-SLAB, and KenPAVE, have been used to

analyze pavements. These programs are successfully in the analysis of pavements with uniform slab thicknesses, multiple layers, different slab sizes, and various other criteria. Although, the 2-D model utilized in this research was an adequate verification method for a single placed layer it was not adequate for the multilayered systems. Therefore, an alternate 3-D model was developed to supplement the analysis of the multi-layered systems. In this research, the analysis package ISLAB2000 was used for the 2-D model and ANSYS was used for the 3-D model.

2.5.1 Modeling of Concrete and Asphalt Layers

In a composite pavement the AC and PCC can be modeled by using eight node elements, also known as brick elements. Elements with a larger number of nodes, i.e. higher order elements, could also be utilized. Using a higher order element, results in an increase of computational resources. To reduce the computational need and maintain accuracy, 8-node brick elements including "extra displacement functions" can be used [17]. Since parasitic shear can result from the assumed displacement functions associated with the formulation of the 8-node solid element, extra displacement function are used to correct for this problem and enable the element to accurately represent the bending effects of the structure. 8-node solid elements with extra displacement functions were used to model the representation of Iowa Highway 13 investigated by this research.

2.5.2 Foundation Modeling Techniques

Pavement analysis and design employs three different types of foundation modeling; liquid, solid, and layered. The majority of finite element programs utilized today are based on the liquid foundation. This is because liquid foundation models require very little computer time to solve.

The force-deflection relationship of the liquid foundation is characterized by an elastic spring. The term "liquid" is used to indicate that the foundation's deformation under a slab is similar to how water deforms under a boat [18]. The liquid foundation is also known as a Winkler foundation which is shown in Figure 2-3.

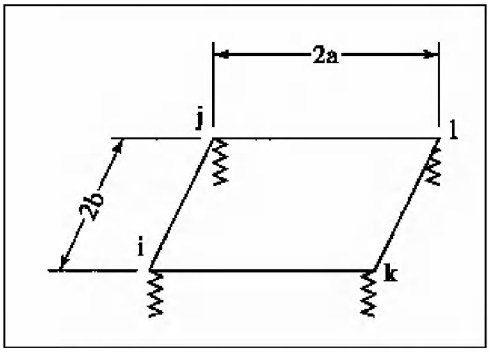

Figure 2-3 Liquid Foundation under a Plate Element

A more realistic type of foundation is the solid foundation also known as the Boussinesq foundation. The deflections of a solid foundation at any nodal point depend on the forces acting at all nodes and not just the forces acting at that point [18]. In the finite element modeling section presented later an 8-noded element was used to represent the solid foundation.

3.0 MODELING OF IOWA HIGHWAY 13

As described in previous sections the purpose of this work is to verify simplified structural analysis methods used in the analysis of multi-layered pavements such as Iowa Highway 13. Although there are several two dimensional (2-D) and three dimensional (3-D) finite element packages available, ISLAB2000 (2-D) and ANSYS (3-D) were chosen for the modeling of the composite pavement. This was due to their availability and time requires for this study.

3.1 Modeling of Composite Pavement for Finite Element Analysis

In order to verify the structural analysis method previously described in Chapter 2, three finite element models representing an "equivalent" plate, an AC/PCC pavement and a PCC/AC/PCC pavement were needed. In the work presented here, two dimensional and three dimensional modeling techniques are used. For the two dimensional modeling of the "equivalent" plate and AC/PCC pavement, the AC and concrete layers are represented by multiple layers of thin plates resting on a Winkler foundation. The foundation's stiffness is designated by the modulus of subgrade reaction (k-value) of the soil. To account for the bond condition at the AC/PCC interface, ISLAB2000 allows for the selection of either fully bonded or completely unbonded.

For the three dimensional modeling, plate and solid elements were used to construct the "equivalent" plate, PCC overlay, AC, PCC base, and soil subgrade. When using solid elements to model the soil subgrade, the k-value is not adequate and needs to be related to the soils elastic modulus (E_S) and its poison's ratio (ν_S). Modeling of the bond condition is done for the fully bonded cases by using common nodes at the interface between the layers. For the unbonded cases, two sets of nodes are utilized at each nodal location. To link these nodes together in the vertical direction the ANSYS program provides the "couple" command. In order to represent an unbonded pavements behavior restraints are applied only in the vertical direction and not in the horizontal directions.

3.1.1 Types of Element Used to Model Iowa Highway 13

The following is a brief description of the type of elements used in the 3-D modeling of the AC/PCC and PCC/AC/PCC pavements.

3.1.1.1 Plate Elements

SHELL63 was chosen to model the "equivalent" plate, an unbonded AC/PCC pavement and the pavement subgrade. It is an element that has both bending and membrane capabilities. Loading can be applied normal to the plane or in-plane. There are six degrees of freedom per node allowing for translations and rotations in the x, y, and z directions. The element permits for a single thickness or is allowed to vary across the element. This element allows for the soil subgrade modulus typically associated with a Winkler foundation to be represented by defining and Elastic Foundation Stiffness (EFS) [19]. This is a more convenient method to model the Winkler foundation instead of individual nodal springs.

Since solid elements do not have the EFS capabilities, the foundation can be modeled by placing a very thin layer of plate elements under the pavement structure. This permits for the effects of a foundation without increasing the stiffness of the pavement.

3.1.1.2 Solid Elements

SOLID45 was chosen for the three dimensional modeling of the various layers in the composite pavement structure. It is an 8-node brick element with 3 degrees of freedom at each node: allowing for displacement in the nodal x-, y- and z-directions. This element has plastic, creep, swelling, stress stiffening, large deflection and large strain capabilities, along

with the capability of representing orthotropic material properties. Additionally, the element is capable of supporting pressures on any surface and concentrated forces at the nodes [19].

Since the element only has 2 nodes along each edge its interpolation functions are linear. Therefore, utilizing the basic 8-node element in analysis will result in constant strains and stresses across the element. This approach is not correct when accounting for bending stresses and the use of a higher order element would produce a more accurate result. The use of higher order elements requires increased computing time for the analysis. This time can be significantly reduced by including extra shape functions in the stiffness formulation of the element [17]. When using SOLID45, ANSYS does provide this option.

3.2 Finite Element Modeling of the "Equivalent" Plate

Modeling of the "equivalent" plate was performed using ISLAB2000 which idealizes the thickness of a slab as multiple layers of thin plates. The thickness of the slab was determined to be 9.69". The "equivalent" plate was also modeled in ANSYS, using a plate element, a single layer of solid elements and two layers of solid elements though the thickness. The foundation for the "equivalent" plate was modeled using a very thin layer of plate elements beneath the plate structure. Results of the various modeling techniques can be seen later in the analysis section of this paper.

3.3 Finite Element Modeling of the Composite System (Iowa Highway 13)

Since the purpose of the analysis presented in this work is to investigate a simplified method for structurally evaluating pavements, it was not necessary to consider the effects of a widening unit as part of the investigation. Therefore, only representative models of Iowa Highway 13 were used for the finite element modeling. The models were constructed as a single 18 ft wide by 70 ft long slab, consisting of either two layers (AC/PCC) or three layers (PCC/AC/PCC). Each layer was constructed with a uniform thickness of 7 inches for the

original PCC, 5 inches for the AC, and 3.5 inches for the PCC Overlay. Pavement variables such as slab size and temperature effects such as curling and warping are not part of this research and will not be taken into consideration.

As previously described, the PCC overlay, AC and bottom PCC layers were meshed using plate and solid elements. Modeling of the AC/PCC pavement using plate elements was constructed using a single layer of elements for both the AC and PCC layer. This was done for the two layer unbonded case only. For all other models constructed with ANSYS the overlay and AC layers were modeled with a single layer of solid elements and the bottom PCC slab was modeled using two layers of solid element though the thickness. To model the soil underneath the pavement two methods were used. The first method was to place a very thin layer of plate elements beneath the pavement structure. The second method was to model the soil using a total depth of 40 inches and four layers of solid elements through the thickness. The modeling technique of the soil using brick elements is shown in Figure 3-1.The effects for the different modeling techniques are shown later in the analysis section of this paper.

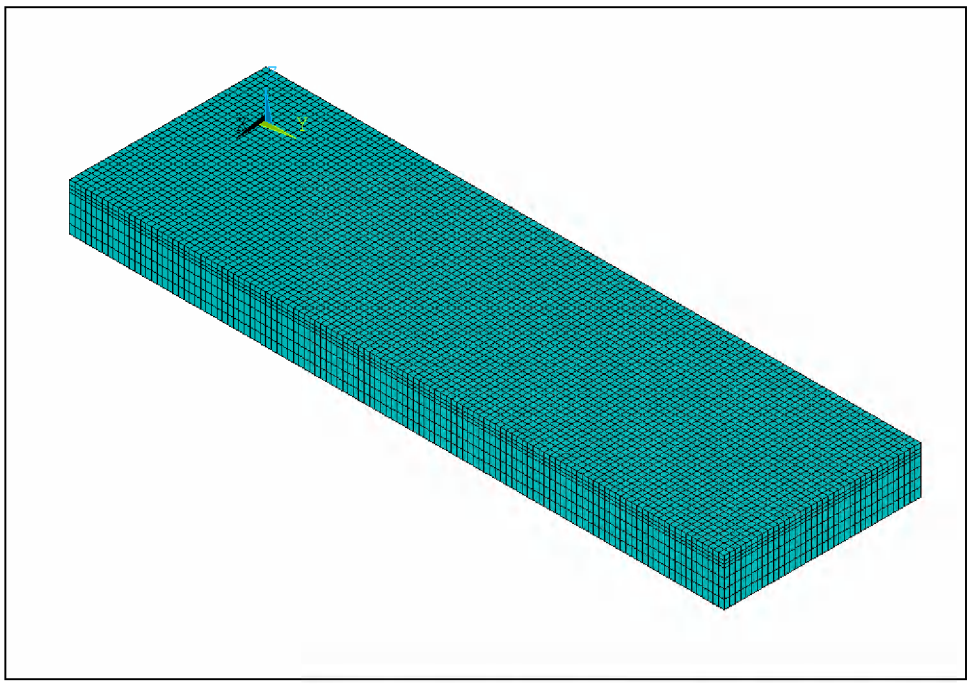

Figure 3-1 Modeling of the Pavement and Soil using Solid Elements

4.0 FIELD EVALUATION OF IOWA HIGHWAY 13

4.1 Visual Survey

Visual surveys of Iowa Highway 13 were performed before and after construction of the overlay. They were conducted prior to construction to evaluate the existing pavement and determine if an unbonded overlay was an adequate rehabilitation method. Surveys conducted after construction focused on the effects of heavy loading and freeze thaw cycles experienced by the pavement.

Results of the preconstruction survey showed that the pavement was in good structural condition with minimal cracking. There were signs of working cracks in the pavement over areas in which culverts were located. Reflective cracking was also evident throughout the roadway. Evidence of a longitudinal crack was found in the AC overlay at the location of the edge of the old PCC slab. This longitudinal crack extended the entire length of the pavement in both the northbound and southbound lanes [1].

Visual surveys performed after construction of the overlay were conducted biannually in the months of October and April. Surveys considered distresses such as longitudinal cracking, transverse cracking, diagonal cracking, fractured panels, and condition of the widening joint. Detail of the distress surveys were documented in the final report [20].

4.2 Nondestructive Deflection Testing

Deflection testing on Iowa Highway 13 was performed by the Iowa DOT with a Foundation Mechanics JILS-20-Falling Weight Deflectometer (FWD). Testing was conducted biannually, once the fall and then again in the spring. FWD testing performed prior to the construction of the overlay was done in the outer wheel path for each lane of the roadway. A single test was done at each location and then repeated at that location for the duration of the project.

The FWD has a load plate with a radius of 6 inches. Nine deflection sensors were spaced at varying distances from the load plate with sensor one located at the center of the plate. A load magnitude of 9,000 pounds was used for the deflection testing. Figure 4-1 shows the location of the sensors in references to the load placement. [1] Air temperature was also monitored and recorded during the deflection testing. Deflection measurements and temperature results taken prior to the overlay are listed in Appendix A. These results were then used to backcalculate the pavement properties of the existing pavement.

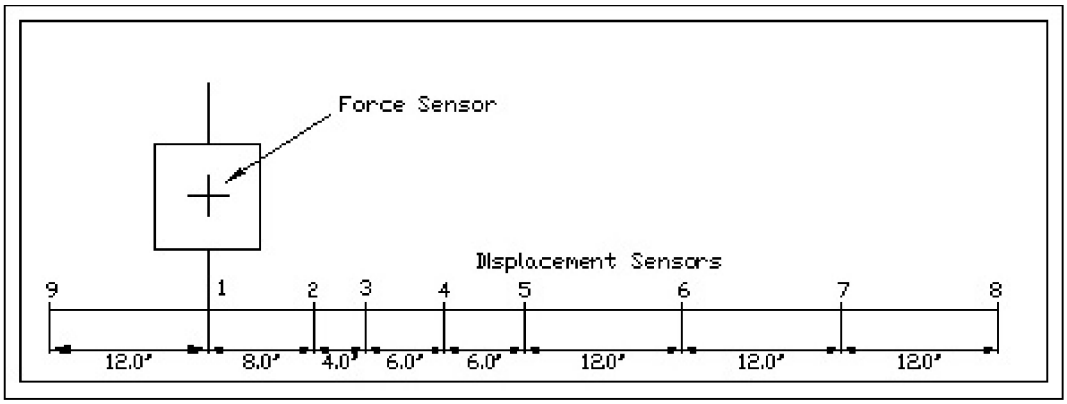

Figure 4-1 Schematic of FWD Deflection Sensors

4.3 Soil Classification

As part of this research project, soil identification was conducted along the 9.6 mile segment of Iowa Highway 13. The soil identification included consultation of the US Department of Agriculture (USDA) soil survey for Delaware County and visual soil classification was performed by the research team. Soil borings were conducted on the shoulder of the roadway approximately 1 foot from the edge of the pavement. A complete list of results from the soil classification can be seen in Appendix B. The summary of the finding from the USDA soil survey and visual classification are summarized below.

4.3.1 Soil Survey Summary

There are three different soil associations located along the 9.6 mile segment of Iowa Highway 13. These associations are the Kenyon-Clyde-Floyd association (green), the Downs-Fayette association (yellow), and the Spillville-Saude-Marshan association (blue) with the predominant association being the Kenyon-Clyde-Floyd association. This can be seen in Figure 4-2. Since the primary association is the Kenyon-Clyde-Floyd association it will be the primary focus of the research and can be described in more detail as Kenyon Loam (83B) and Clyde-Floyd Complex (391B) [21].

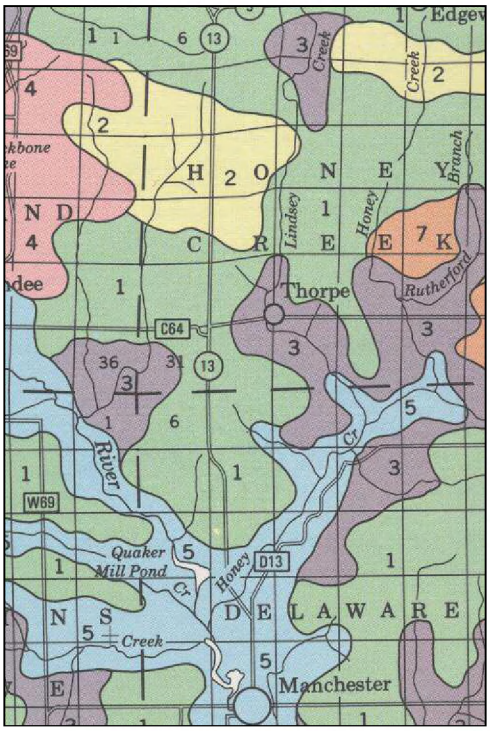

Figure 4-2 Iowa Highway 13 Soil Associations

Kenyon Loam (83B) is located on side slopes in the uplands and on long convex ridge tops. This soil is gently sloping and moderately well drained. A Kenyon Loam subsurface profile can be seen below.

- A surface layer of black loam approximately 7 inches thick and contains roughly 3 to 4 percent organic mater

- A subsurface layer of black and very dark grayish brown loam approximately 10 inches thick
- A subsoil of loam approximately 37 inches thick, with
    - An upper section of brown friable loam
    - A lower section of dark yellowish brown and yellowish brown, mottled, firm loam
- A substratum of mottled yellowish brown and grayish brown loam

Kenyon Loam is classified under American Association of State Highway Transportation Officials (AASHTO) as an A-6. Under the Unified Soil Classification System (USCS) this soil is classified as a CL.

The Clyde-Floyd Complex (391B) is located in drainage ways on glacial uplands. These soils are gently sloping and poorly drained. The Clyde soils have a slope of less than 2 percent and are located in the lowest part of the drainage way. Located in bands bordering the Clyde soils, Floyd soils have a slope of 1 to 4 percent. These two soils are not mapped separately due the complex mixing of the areas in which they occur.

A Clyde-Floyd Complex subsurface profile contains:

- Clyde soils
    - A surface layer of black loam approximately 9 inches thick
    - A subsurface layer is black clay loam approximately 14 inches thick
    - A subsoil is approximately 18 inches thick, with
        - An upper section of gray, mottled, friable loam
        - A middle section of mottled gray and yellowish brown, friable loam with a sandy stratum of approximately 1 inch thick
        - A lower section of gray, mottled, firm loam
    - A substratum of mottled gray and yellowish brown loam
- Floyd soils
    - A surface layer of black loam approximately 9 inches thick
    - A subsurface layer is black and very dark brown loam approximately 13 inches thick

- A subsoil is mottled loam approximately 18 inches thick, with
  - An upper section of dark grayish brown and friable
  - A middle section of olive brown and light olive brown loam
  - A lower section of grayish brown firm loam
- A substratum of mottled grayish brown loam

The Clyde-Floyd Complex is classified under American Association of State Highway Transportation Officials (AASHTO) as A-6 and A-7 soils. Under the Unified Soil Classification System (USCS) these soils can be classified as an OH, MH, ML, OH, CL, SM, SM-SC, and/or SC [21].

4.3.2 Visual Soil Classification Survey

At various depths, soil boring revealed yellowish brown sandy clay with gray mottling. Also, brown to very dark brown sandy clay or silt was also found. The expected soil conditions identified by the USDA soil survey correlated with the results of the visual classification.

5.0 DATA ANALYSIS

The purpose of this research is to investigate and verify existing methodologies related to the analysis and design of PCC overlays. One of those methodologies, developed by Ioannides, proposes that stresses determined from an imaginary "equivalent" plate can be used to calculate deflections and stresses within a composite pavement. Research presented here uses finite element modeling, based on an existing pavement structure, to verify these calculated results

.

Before deflections and stresses can be determined, material properties of the existing pavement are calculated. A Falling Weight Deflectometer was used to perform the deflection testing for this research project. Measurements taken from sensors located at 0, 12, 24, and 36 inches are used to determine the cross sectional area of the deflection basin, modulus of subgrade reaction (k_S), and the elastic modulus of the PCC slab (E_{PCC}). Corrections were made to the maximum deflection under the load to account for slab size effects and compression in the AC due to loading. These values are then used to develop the various models used in this research.

5.1 Determination of Properties for AC/PCC and PCC/AC/PCC Pavements

5.1.2 AC Elastic Modulus

A large portion of the total measured deflection of an AC/PCC pavement can be attributed to the vertical compression experienced by the AC layer under the FWD load. To determine the amount of compression in the AC layer the AC elastic modulus (E_{AC}) is calculated. The method outlined below uses the Asphalt Institute's (AI) equation for the AC elastic modulus [22]. Shown in equation 1, this equation is a function of mix characteristics, mix temperature, loading frequency, and is considered to be very reliable for dense-graded AC mixes made up of gravel or crushed stone aggregates [23].

$$\log E_{AC} = 5.553833 + 0.028829\left(\frac{P_{200}}{F^{0.17033}}\right) - 0.03476 * V_V$$
$$+ 0.070377 * \eta + 0.000005 * T_{AC}^{(1.3+0.49825*\log F)} * P_{AC}^{0.5} - \left(\frac{0.00189}{F^{1.1}}\right) \quad (1)$$
$$* T_{AC}^{(1.3+0.49825*\log F)} * P_{AC}^{0.5} + 0.931757 * \left(\frac{1}{F^{0.02774}}\right)$$

Where,

E_{AC} = elastic modulus of AC, psi

P_{200}= percent aggregate passing the No. 200 sieve

F = 18 Hz for the FWD load duration of 25 to 30 milliseconds

V_v = percent air voids

P_{AC} = asphalt content, percent by weight of mix

T_{AC}= mean AC mix temperature at 1/3 depth, ºF

η = absolute viscosity at 70ºF, 10^6 poise

5.1.3 Effects of temperature on the AC elastic modulus

During FWD testing the temperature of the AC layer is measured in order to account for the variability of the AC resilient modulus during testing. Monitoring the AC temperature can be done by drilling a hole to the mid-depth of the AC layer, inserting liquid, and a temperature probe [4]. An alternate method to determine the temperature of the AC using the mean monthly air temperature was developed by Witczak and is shown below [22].

$$T_{AC} = MMAT\left(1 + \frac{1}{z+4}\right) - \frac{34}{z+4} + 6 \quad (2)$$

Where,

T_{AC} = mean temperature of the AC layer

MMAT = mean monthly air temperature

z = 1/3 depth from the surface of the AC, inches

5.1.4 Corrections for Determining the In Situ AC Elastic Modulus

The above equation for the elastic modulus of the AC is typically applied to new mixes. In situ AC mixes over time, can experience asphalt hardening causing a higher modulus value. On the other hand, if AC pavements have experienced large amounts of deterioration a lower modulus value will result [4]. The value for the AC modulus calculated using equation 1, is adjusted for aging using the following equations developed by Ullidtz. Equation 3 is used to determine an aged $Pen_{25°C}$ in which $Pen_{25°C}$ is the penetration of the binder at 25°C (77°F) [22].

$$\text{aged } Pen_{25°C} = 0.65 * \text{original } Pen_{25°C} \tag{3}$$

If there is not sufficient enough information to determine the absolute viscosity needed for equation 1, the following relationship shown in equation 4 [22] is used.

$$\eta = 29508.2 * \left(aged \quad Pen_{25°C} \right)^{-2.1939} \tag{4}$$

5.1.5 Deflection of the Existing PCC Slab

Using the elastic modulus of the AC, the amount of vertical compression in the AC layer is calculated. Measured deflections at d_0 are significantly larger when there is no bond between the AC layer and the PCC layer. However, the actual bond condition is typically unknown. As part of this research both bond conditions are considered. Therefore the following two equations are used to calculate the degree of compression experienced by the AC layer [4].

AC/PCC Bonded

$$d_{0_{compress}} = -0.0000328 + 121.5006 * \left(\frac{D_{ac}}{E_{ac}} \right)^{1.0798} \tag{5}$$

AC/PCC Unbonded

$$d_{0_{compress}} = -0.00002132 + 38.6872 * \left(\frac{D_{ac}}{E_{ac}} \right)^{0.94551} \quad (6)$$

Where,

$d_{0\,compress}$ = AC compression at center of load, in

D_{ac} = AC thickness, in

E_{ac} = AC elastic modulus, psi

After the compression of the AC layer is determined, the calculated value is subtracted from the deflections measured at d_0 by the FWD, resulting in the actual deflection of the existing PCC layer (d_{0PCC}) [4].

$$d_{0PCC} = d_0 - d_{0compress} \quad (7)$$

Where,

$d_{0compress}$ = vertical compression of the AC layer, in

d_0 = maximum deflection at center of load plate, in

d_{0PCC} = deflection of the PCC layer at the center of the load plate, in

5.1.6 Deflection Basin of the PCC ($AREA_{PCC}$)

Now that the influence of the AC layer has been removed from the deflection measurements, the area of the deflection basin of the PCC slab is determined using equation 8 [4].

$$AREA_{PCC} = 6 * \left(1 + 2 * \left(\frac{d_{12}}{d_{0_{PCC}}} \right) + 2 * \left(\frac{d_{24}}{d_{0_{PCC}}} \right) + \left(\frac{d_{36}}{d_{0_{PCC}}} \right) \right) \quad (8)$$

Where,

$AREA_{PCC}$ = area of the deflection basin, in

d_{0PCC} = deflection of the PCC layer at center of load plate, in

d_i = deflection at 12, 24, and 36 inches from the center of the load plate, in

Results from the AREA calculation are then used to estimate a radius of relative stiffness (l) which is defined as the ratio of the PCC slab to the stiffness of its foundation. These results are then used to calculate the modulus of subgrade reaction (k_S). The following equation was developed by Hall to calculate the radius of relative stiffness (l) as a function of the deflection basin [24].

$$l = \left[\frac{\ln\left(\frac{36 - AREA_{PCC}}{1812.279} \right)}{-2.559} \right]^{4.387} \tag{9}$$

5.1.7 Slab Size Correction

The above backcalculation procedure uses Westergaard's equation for deflection of an infinite plate on a dense liquid foundation. However, actual PCC slabs are too small to approximate infinite behavior. Therefore, adjustments to the deflection measured at d_0 and the calculated radius of relative stiffness are applied [25]. To determine if the adjustments are necessary the ratio of L/l is calculated where L is the least slab dimension. If the L/l resulting value is less than eight, the following corrections are applied to the maximum deflection in the PCC slab and calculated radius of relative stiffness [4].

$$AF_{d_0} = 1 - 1.0687 * e^{-0.66914 * \left(\frac{L}{l}\right)^{0.84408}} \tag{10}$$

$$AF_l = 1 - 5.29875 * e^{-2.17612 * \left(\frac{L}{l}\right)^{0.49895}} \tag{11}$$

$$d_{0adj.} = AF_{d_0} * measured\ d_0 \tag{12}$$

$$l_{adj.} = AF_l * calculated\ l \tag{13}$$

AF_{d0} = adjustment factor for the measured d_0

AF_l = adjustment factor for the radius of relative stiffness

d_{0adj} = adjusted maximum deflection d_0, in

l_{adj} = adjusted radius of relative stiffness

5.1.8 Dynamic Modulus of Subgrade Reaction

The radius of relative stiffness is then used to calculate the modulus of subgrade reaction using Westergaard's deflection equation and the adjusted values described above. The modulus value determined from the FWD deflection measurements is considered to be a dynamic modulus. The calculated dynamic modulus is about twice that of a modulus value determined from a static bearing plate test. In typical pavement design, modulus values are considered to be static. Therefore, values determined from this research should be halved if used for design purposes [4].

$$k_S = \left(\frac{P}{8 * d_{0adj} * l_{adj}^{\ 2}}\right)\left\{1 + \left(\frac{1}{2\pi}\right)\left[\ln\left(\frac{a}{2 * l_{adj}}\right) + \gamma - 1.25\right]\left(\frac{a}{l_{adj}}\right)^2\right\} \qquad (14)$$

where,

k_S = effective modulus of subgrade reaction, pci

d_{0adj} = adjusted maximum deflection d_0, in

l_{adj} = adjusted radius of relative stiffness

P = FWD load, pounds

γ = Euler's constant, 0.57721566490

a = load radius, 5.9 inches for the FWD

5.1.8.1 Relationship between a liquid and solid foundation

For the finite element modeling previously described, two types of foundations were used for modeling the soil. The ISLAB models use a liquid elastic foundation and the ANSYS models use both liquid elastic and an elastic solid foundation. When modeling a liquid elastic foundation the modulus of subgrade reaction (k_S) value is directly inputted into the program. Modeling of the elastic solid foundation required values such as the elastic modulus (E_S) and poison's ratio (ν_S) of the soil. Therefore, a relationship a relationship between the modulus of subgrade reaction and the elastic modulus was needed.

It is recommended by Vesic and Saxena (1974) that when computing stresses the following equation 15 be used to relate k_S and E_S. If the deflection is to be found it is recommended that only 42% of the solution from equation 15 be used. However, Huang and Sharpe (1989) determined that equation 15 is only applicable when the load is located on the interior of the slab and recommend equation 16 for loads located on the edge [18].

$$k_S = \left(\frac{E_S}{E_{PCC}}\right)^{1/3} \frac{E_S}{(1-\nu_s^2)h_{PCC}} \tag{15}$$

$$k_S = 1.75\left(\frac{E_S}{E_{PCC}}\right)^{1/3} \frac{E_S}{(1-\nu_s^2)h_{PCC}} \tag{16}$$

k_S = effective modulus of subgrade reaction, pci
E_S = elastic modulus of the soil, psi
ν_S = poison's ratio of the soil, psi
E_{PCC} = elastic modulus of the PCC slab, psi
h_{PCC} = thickness of the PCC slab, inches

An alternative equation known as the reduced Vesic equation may also be used when relating the modulus of subgrade reaction to the elastic modulus of the soil. This equation is shown in equation 17 in which B is the diameter of the bearing plate, typically taken as 30 inches. The reduced Vesic equation is impartial to the placement of a load on a pavement surface and produces comparable results to the above mentioned equations [26].

$$k_S = \frac{E_S}{B\left(1-\nu_s^2\right)} \tag{17}$$

k_S = effective modulus of subgrade reaction, pci

E_S = elastic modulus of the soil, psi

ν_S = poison's ratio of the soil, psi

B = diameter of the bearing plate or 30 inches

In the Field Evaluation section of this report it was shown that a significant portion of the soils located along Iowa Highway 13 were classified as CL type soils. The subgrade modulus of reaction for these types of soils can range from 125 pci to 225 pci. Therefore, the calculated k_S value of 150 pci is acceptable. The poison's ratio for these types of soils can range from 0.3 to 0.5 [18]. In this research the averaged value of 0.4 is used for the Poisson's ratio. A table of the calculated soil elastic moduli can be seen in Table 5-1.

Table 5-1 Elastic Modulus of the Soil Summary

	Unbonded	Bonded
Center Load		
E_S, psi	6790	7100
$E_{S\ 42\%}$, psi	2850	2980
Edge Load		
E_S, psi	4460	4670
Reduced Vesic		
E_S, psi	3970	3970

5.1.9 Existing PCC Elastic Modulus

With the modulus of subgrade reaction determined the elastic modulus of the PCC slab may be calculated [27].

$$E_{PCC} = \frac{12 * \left(1 - \nu_{PCC}^2\right) * k * l^4}{D_{PCC}^3} \quad (18)$$

where,

E_{PCC} = estimated elastic modulus of the existing PCC, psi

ν_{PCC} = Poisson's ratio of the PCC

k = effective modulus of subgrade reaction, pci

l = adjusted radius of relative stiffness

D_{PCC} = thickness of the existing PCC slab, in

This backcalculation procedure is completed at each station where the FWD load is dropped over the length of the project. Since the PCC moduli vary considerably over the length of the project. Deflection values that produce AREA values larger than 36 are not used in calculations of the PCC moduli. In order to add a factor of safety to the design and to address the spread that can be seen in the calculated PCC modulus, a cumulative percentage plot is used [4]. Once the PCC moduli are backcalculated from the above procedure, a histogram is created using a reasonable grouping interval. The cumulative percentage is then calculated from the histogram data using the following equation:

$$\frac{\#of\ \mathrm{mod}ulli \le current\,\mathrm{int}erval}{total\#of\ \mathrm{mod}uliivalues} = \text{Cumulative Percentage} \quad (20)$$

The results are then plotted with the moduli values on the x-axis and the percentage on the y-axis. Depending on how conservative the engineer wants to make the design, a percentage is selected. Three percentages should be used depending on the level of design sought: 60% should be used for a lean design, 75% should be used for a middle of the road design, and 85% should be used for a conservative design [2].

Information provided by the IDOT estimated the compressive strength of the whitetopping layer to be 4500 psi. A complete table of results from the above described

procedure is located in Appendix C. A summary of the existing AC and PCC properties are shown in Table 5-2.

Table 5-2 Summary of Material Properties

	Unbonded E_{PCC}, psi	Bonded E_{PCC}, psi
65%	2600000	2300000
75%	3700000	3100000
85%	4500000	3750000
Elastic Modulus of the AC, psi	1354680	
Elastic Modulus of the PCC Overlay, psi	3823680	

5.2 Determination of Stresses using Ioannides "Equivalent" Plate Method

The "equivalent" plate theory was developed by Ioannides et al. as a way to evaluate the contribution of the modulus when a PCC slab is placed on top of a stabilized base [5]. In this work, this theory is applied to an AC/PCC pavement. It is proposed that stresses determined from an imaginary "equivalent" plate can be used to determine the stresses within the composite plate that it represents. First an equivalent thickness (h_e) must be determined using properties from the actual composite structure. In order to determine the thickness the assumptions outlined in section 2.5.1 must be maintained and a decision on whether the AC is fully bonded or completely unbonded from the PCC layer. Stresses within the "equivalent" plate along with its deflection are determined using either Westergaard's equations or finite element analysis. This "equivalent" stress is then used to calculate stresses at the various interfaces of the composite pavement.

5.2.1 Evaluation of the "Equivalent" Plate for an Unbonded AC/PCC Pavement

If the AC and PCC layers are not bonded, the equation to calculate thickness of the equivalent "plate" is rather simple. For equation 20 it was assumed that the properties in the equivalent plate were equal to the properties of the AC layer.

$$h_e = \left[D_{AC}^3 + \frac{E_{PCC}}{E_{AC}} * D_{PCC}^3 \right]^{(1/3)} \tag{20}$$

where,

h_e = equivalent thickness of the existing pavement, in
D_{AC} = thickness of the AC layer, in
D_{PCC} = thickness of the PCC layer, in
E_{AC} = elastic modulus of the AC, psi
E_{PCC} = elastic modulus of the PCC, psi

The thickness and stresses determined for the "equivalent" plate (σ_e) are then used to calculate the maximum bending stress in the bottom of AC layer (σ_{AC}) using equation 21. The stresses in the bottom of the PCC layer (σ_{PCC}) are then determined using equation 22 [5].

$$\sigma_{AC} = \frac{D_{AC}}{h_e} * \sigma_e \tag{21}$$

$$\sigma_{PCC} = \frac{D_{PCC}}{E_{AC}} * \frac{E_{PCC}}{E_{AC}} * \sigma_{AC} \tag{22}$$

5.2.2 Evaluation of the "Equivalent" Plate for a Bonded AC/PCC Pavement

If the AC and PCC layers are bonded, the neutral axis of the composite plate is calculated before the equivalent thickness is determined. For equation 23 it was assumed that the properties in the equivalent plate are equal to the properties of the PCC layer [5].

$$x = \frac{E_{PCC}D_{PCC}\frac{D_{PCC}}{2} + E_{AC}D_{AC}\left(D_{PCC} + \frac{D_{AC}}{2}\right)}{E_{PCC}D_{PCC} + E_{AC}D_{AC}} \tag{23}$$

where,

x = distance to the neutral axis, in
D_{AC} = thickness of the AC layer, in
D_{PCC} = thickness of the PCC layer, in
E_{AC} = elastic modulus of the AC, psi
E_{PCC} = elastic modulus of the PCC, psi

After the location of the neutral axis in determined the "equivalent" thickness of the plate is calculated.

$$h_e = \left\{ \begin{array}{l} D_{PCC}^3 + \frac{E_{AC}}{E_{PCC}} D_{AC}^3 \\ +12\left[\left(x - \frac{D_{PCC}}{2}\right)^2 D_{PCC} + \frac{E_{AC}}{E_{PCC}}\left(D_{PCC} - x + \frac{D_{AC}}{2}\right)^2 D_{AC}\right] \end{array} \right\}^{(1/3)} \tag{24}$$

where,

D_{AC} = thickness of the AC layer, in
D_{PCC} = thickness of the PCC layer, in
E_{AC} = elastic modulus of the AC, psi
E_{PCC} = elastic modulus of the PCC, psi

The thickness and stresses determined for the "equivalent plate (σ_e) are then used to calculate the maximum bending stress in the top of the PCC layer (σ_{PCC}) using equation 25. Stresses in the top of the AC layer (σ_{AC}) are then determined using equation 26 [5].

$$\sigma_{PCC} = \frac{2(D_{PCC} - x)}{h_e} * \sigma_e \tag{25}$$

$$\sigma_{AC} = \sigma_{PCC}\left(\frac{E_{AC}}{E_{PCC}}\right)\left(\frac{D_{AC} + D_{PCC} + x}{x}\right) \tag{26}$$

5.3 Comparison of ANSYS and ISLAB2000 with Ioannides "Equivalent" Plate Method

As mentioned in the previous section an "equivalent" plate may be used to represent a composite AC/PCC pavement in which the properties of the plate are based on the properties of the composite structure. The equivalent stresses with in the plate can then be used to determine the maximum displacement and stresses with in the layers of the composite AC/PCC pavement. Finite element analysis was used to verify this statement. In order to minimize the amount of work for calculations and the finite element analysis, the following properties were used; mesh size = 6 in x 6 in, $E_{PCC\ Overlay}$ = 3,823,680 psi, E_{AC} = 1,354,680 psi, E_{PCC} = 3,100,000 psi, k_S = 150 pci, E_S = 3,970 psi and ν_S = 0.40. Also, a 9 kip load was distributed over a 144 sq. in. area located in the center of the slab.

5.3.1 Evaluation of Westergaard's Equations for an Unbonded AC/PCC Pavement

In this work Westergaard's equations for deflection and stress were chosen to determine the behavior of the "equivalent" plate. Finite element analyses were performed to verify Westergaard's equations. Using properties and methods described in previous sections the thickness for the "equivalent" plate was determined to be 9.69 inches. A summary of the results are shown in Table 5-3. Calculations, deflection, and stress contours for the ISLAB2000 model can be seen in Appendix D.

Table 5-3 Summary of the "Equivalent" Plate Verification

	Westergaard	ISLAB2000 (2-D)	ANSYS (3-D)		
			Shell Element	Single Solid Element	2 Layered Solid Elements
Displacement (in)	0.0083	0.0085	0.0035	0.0090	0.0089
Stress (σ_{top} psi)	-133	-138	-131	-125	-128
Stress (σ_{bottom} psi)	133	138	131	120	107

The results showed that Westergaard's equations are a valid method for determining the stresses and deflection in a homogeneous plate of uniform thickness. The 2-D analysis resulted in deflections with less than a one percent difference. However the stresses were 3% higher than Westergaard's results. Of the 3-D analyses, use of shell elements produced the least amount of discrepancy in the stress distribution, but there was a 58% difference in the amount of deflection when compared to Westergaard. Also, when compared to Westergaard, the use of two layered elements produced a 7% difference in deflection and a 19% difference in the averaged stress distribution.

5.3.2 Application of the "Equivalent" Plate Method to an AC/PCC Pavement

Using Ioannides "equivalent" plate methodology as described in section 5.2.1, displacement and stresses in the top and bottom of each layer are determined for both an unbonded and bonded AC/PCC pavement [5]. Calculations for the Ioannides method are shown in Appendix E. These results were then compared to deflections and stresses determined from finite element analyses. A summary of the deflections for the unbonded AC/PCC pavement can be seen in Table 5-4.

Table 5-4 Summary of Displacements in the Unbonded AC/PCC Pavement

	ISLAB2000	ANSYS: PLATE Elements	ANSYS: SOLID Elements	Ioannides
Displacement (in)	0.0088	n/a	0.0086	0.0083

When compared to Ioannides the deflection results showed that ISLAB2000 produced a difference of 6%. ANSYS resulted in only a 4% difference when compared to Ioannides method. A graphical output from the ANSYS program, seen in Figure 5-1 shows an example of the deflection.

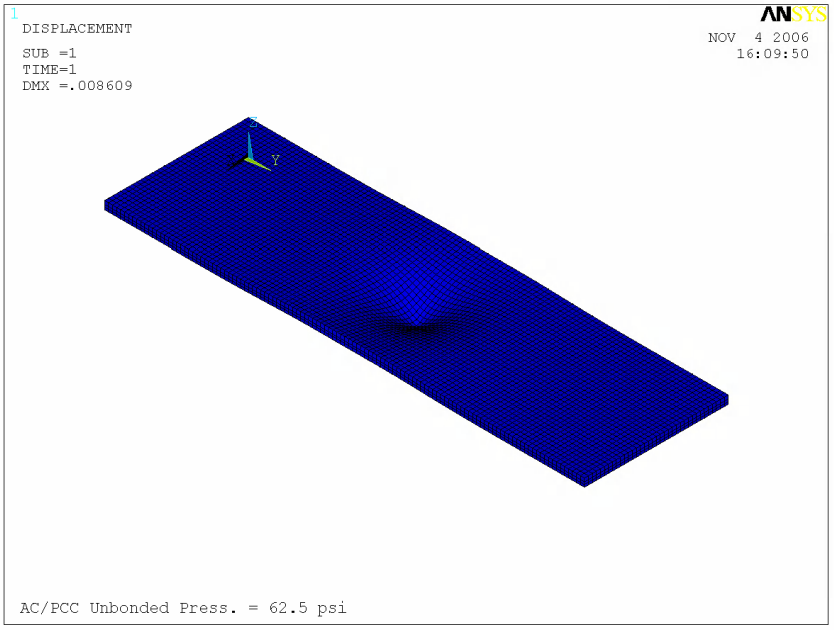

Figure 5-1 Deflection of the Unbonded AC/PCC Pavement

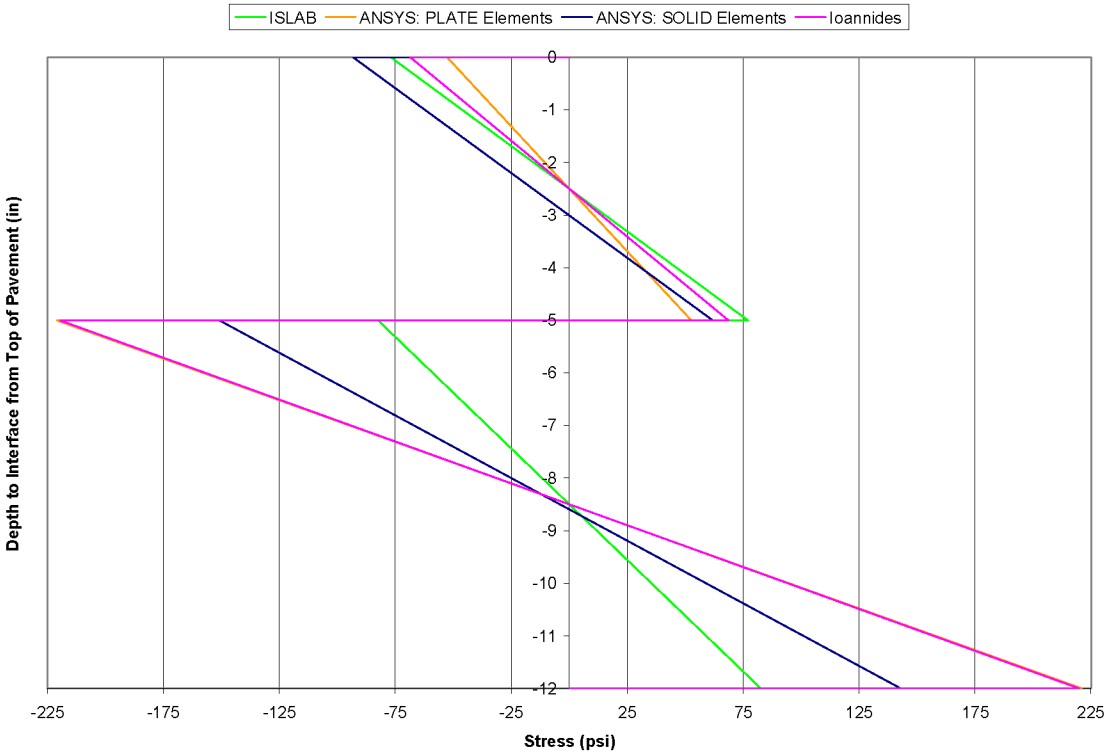

Figure 5-2 Summary of Stress Distributions in the Unbonded AC/PCC Pavement

Figure 5-2 shows the resulting stress distribution for the unbonded AC/PCC pavement. The 2-D model using ISLAB2000 produced 62% lower stresses for the PCC layer when compared to Ioannides solution. When comparing Ioannides results to the ISLAB2000 model, the Ioannides method produced 12% lower stresses in the top AC layer. The 3-D model using a layer of plate elements to model each consecutive layer produced a 1% difference in stress for the PCC layer when compared to Ioannides solution. However, the actual behavior of a pavement is more closely resembled by that of the solid element model. When comparing Ioannides results to the solid element model, the Ioannides method produced 30-35% higher stresses in the top of the AC layer and in the PCC layer.

Table 5-5 Summary of Displacements in the Bonded AC/PCC Pavement

	ISLAB	ANSYS: SOLID Elements	Ioannides
Displacement (in)	0.0053	0.0052	0.005

For the bonded case in Table 5-5, the deflection results showed that ISLAB2000 produced a difference of 6% when compared to Ioannides. ANSYS resulted in only a 4% difference when compared to Ioannides method.

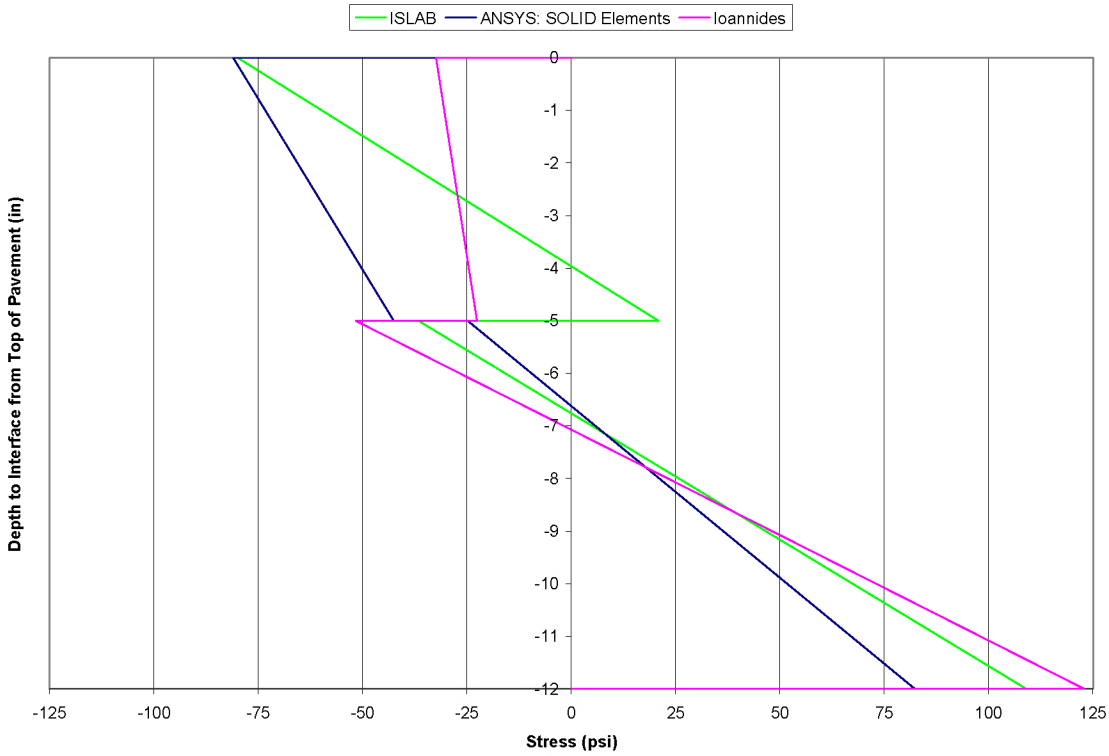

Figure 5-3 Summary of Stress Distributions in the Bonded AC/PCC Pavement

Figure 5-3 shows the resulting stress distributions for the bonded AC/PCC Pavement. The 2-D model using ISLAB2000, produced a range of 11-29% difference in stress for the PCC layer when compared to Ioannides solution. When comparing Ioannides results to the ISLAB2000 model, the Ioannides method produced 59% lower stresses in the top AC layer. The 3-D model using solid elements to model each consecutive layer produced 33% lower

stresses in the bottom of the PCC layer and 52% lower stresses for the top of the PCC layer when compared to Ioannides solution. The Ioannides method produced 60% lower stresses in the top AC layer when compared to the solid element model.

5.3.3 Application of the "Equivalent" Plate Method to a PCC/AC/PCC Pavement

Using the methodologies outlined in section 5.2.1 and applying the assumptions given in section 2.5.1 a "equivalent" plate solution for a PCC overlaid AC/PCC pavement was developed. For the calculations of the "equivalent" thickness for both the unbonded and bonded interface conditions it was assumed that the properties in the equivalent plate were equivalent to the properties of the PCC Overlay. The resulting equations and calculations are shown in Appendix F. The 2-D finite element program did not allow for the modeling of the three layered pavement. Therefore, only 3-D finite element analyses were performed to investigate the results of the modified Ioannides method.

Table 5-6 Summary of Displacements in the Unbonded PCC/AC/PCC Pavement

	ISLAB	ANSYS: SOLID Elements	Ioannides
Displacement (in)	n/a	0.0073	0.0077

Table 5-6 shows the deflections determined by the Ioannides method and ANSYS. When compared to Ioannides the deflection results showed that ANSYS produced only a 6%. The resulting stress distributions can be seen in Figure 5-4.

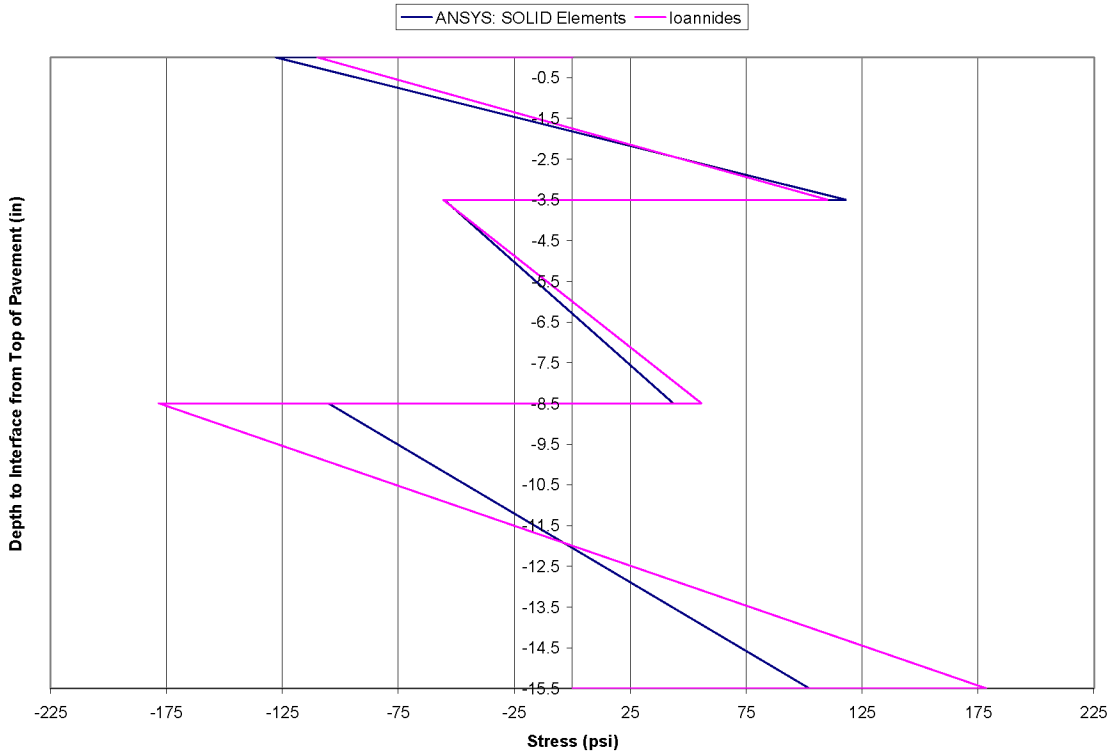

Figure 5-4 Summary of Stress Distributions in the Unbonded PCC/AC/PCC Pavement

Figure 5-2 shows the resulting stress distribution for the unbonded PCC/AC/PCC pavement. The 3-D model using ANSYS, produced 16% higher stresses for the PCC overlay when compared to Ioannides solution. When comparing Ioannides results to the ANSYS model, the Ioannides method produced 22% higher stresses in the bottom of the AC layer. The 3-D model produced a 40% difference in stresses for the lower PCC layer when compared to Ioannides solution.

Table 5-7 Summary of Displacements in the Bonded PCC/AC/PCC Pavement

	ISLAB	ANSYS: SOLID Elements	Ioannides
Displacement (in)	n/a	0.0028	0.0028

Table 5-7 shows the deflections determined by the Ioannides method and ANSYS. When compared to Ioannides the deflection results showed that ANSYS produced only a 1%. The resulting stress distributions can be seen in Figure 5-5.

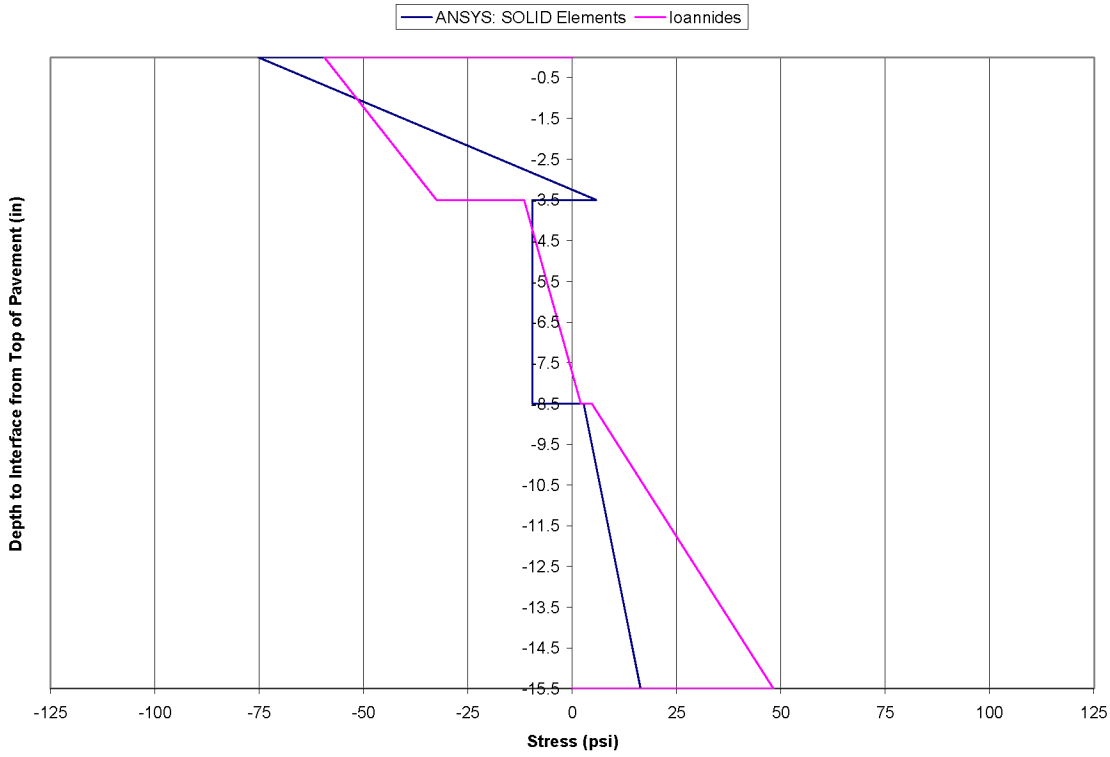

Figure 5-5 Summary of Stress Distributions in the Bonded PCC/AC/PCC Pavement

Figure 5-5 shows the resulting stress distribution for the bonded PCC/AC/PCC pavement. The 3-D model using ANSYS, produced 26% higher stresses for the top of the PCC overlay when compared to Ioannides solution. When comparing Ioannides results to the ANSYS model, the Ioannides method produced 17% higher stresses in the top of the AC layer. The 3-D model produced a 66% difference in stresses in the bottom of the lower PCC layer when compared to Ioannides solution.

6.0 SUMMARY, CONCLUSION, AND RECOMMENDATIONS

6.1 Summary

Iowa is one of few states with a large number of PCC pavements. Many of theses pavements have exceeded their design life and are in need of rehabilitation. One method of rehabilitation is the PCC overlay. In order to improve the design process of overlays many states such as Iowa and Colorado have sponsored research projects such as Iowa Highway 13.

The usage of PCC overlays results in a behavior that is uniquely different from all other pavements. The complex behavior of the composite pavement is difficult to evaluate and much effort has gone into developing guidelines in order to evaluate these pavements accurately. Many of these guidelines incorporate guidelines for typical pavement design of a single placed layer. On method was the application of an "equivalent" plate to represent the actual behavior of the composite structure. In addition to these methods finite element analysis has also become a useful tool in the design of PCC overlays.

In order to investigate how the single placed layer guidelines could be applied to a composite pavement system, finite element modeling was utilized. Solid and shell elements were use to construct the various pavement layers. In addition these elements were used to model the subgrade under the pavement.

To aid in the evaluation of Iowa Highway 13 field investigation were performed. As part of the field investigation visual distress surveys and deflection data collection was performed to asses the condition of the pavement. Soils boring were also conducted to confirm the soil classification of the USDA soil survey.

Before the finite element modeling could be performed properties of the individual pavement layers and soil were calculated using AI's equation for the AC modulus and the backcalculation method developed by Hall and Darter [4]. The properties were input into the

finite element programs for analysis and used to calculate an "equivalent" thickness for the representative plate of the composite pavement. Stresses calculated for the "equivalent" plate were then used to backcalculate stresses in the individual layers of the two composite structures. The closed form solutions were then compared to the results from the finite element analysis.

6.2 Conclusions

The following are some conclusions made during analysis of the composite pavement on Iowa Highway 13:

- The backcalculation procedure developed by Hall and Darter for determining pavement properties is an acceptable method for the determination of soil modulus of subgrade reaction
- Westergaard's equation are a valid method for determining stresses and deflections of pavement slab of uniform properties and thickness
- Deflections determined by finite element analysis for the composite pavements coincide with deflections calculated for their respective "equivalent" plate
- Composite pavements with fully bonded layer experience lower stresses and deflections than composite pavements whose layers are unbonded which verifies already established conclusions

6.3 Future Research Recommendations

The following are recommendations for future study:

- Further investigation into discrepancies between the different methods used to determine the stress distribution of the composite pavement
- Finite element analysis using variable element sizes and types to determine their effects on the resulting stress distribution

- Geometry of the loaded area, how much discrepancy is there between load distribution over a square area such as that used in finite element analysis verses distribution over a circular area assumed by Westergaard
- Development of more precise methods to determine materials properties of the soil such as the elastic modulus and poison's ratio.

APPENDIX A

Table A-1 Northbound Lane Preconstruction FWD Data (Performed on 5/21/2002 on Previous Existing AC Roadway Surface)

TS #	Lane	Station	Load (kip)	Sensor Number / Location									Pav't Temp
				1	2	3	4	5	6	7	8	9	
				d_0	d_8	d_{12}	d_{18}	d_{24}	d_{36}	d_{48}	d_{60}	d_{12}	
1	NB	43+02	9.06	4.75	3.91	3.67	3.49	3.25	2.76	2.3	1.79	3.56	53.1
2	NB	52+94	9.17	5.53	5.43	5.25	4.99	4.68	4.05	3.41	2.79	4.99	53.5
3	NB	63+03	9.06	6.59	5.74	5.4	4.96	4.51	3.62	2.87	2.21	5.75	53.8
4	NB	73+08	9	7.55	7.41	7.24	6.92	6.52	5.6	4.66	3.75	7.21	53.5
5	NB	83+13	8.89	7.43	7.31	7.29	7.18	7.05	5.57	4.32	3.24	6.64	54.2
6	NB	93+00	8.79	10.52	9.53	9.21	8.66	8.26	7.12	5.85	4.45	9.3	53.5
7	NB	103+09	8.65	7.52	7.13	6.79	6.29	5.86	4.84	3.9	3.31	5.94	54.6
8	NB	113+27	8.97	6.39	5.97	5.86	5.61	5.34	4.67	3.95	3.28	5.77	54.2
9	NB	123+09	8.78	6.65	6.36	6.23	5.91	5.58	4.81	4.01	3.26	5.96	54.2
10	NB	133+03	8.8	3.78	3.66	3.58	3.44	3.3	2.99	2.69	1.71	3.29	53.8
11	NB	143+00	8.81	3.37	3.13	2.96	2.81	2.69	2.38	2.07	1.77	2.88	52.4
12	NB	152+80	8.83	6	5.24	5.06	4.89	4.65	4.06	3.45	2.85	5.01	55.7
13	NB	163+02	8.78	7	6.6	6.3	5.96	5.38	4.57	3.79	3.09	5.47	55.7
14	NB	173+12	8.8	6.71	5.79	5.41	5.04	4.71	3.85	3.15	2.44	5.32	54.6
15	NB	186+22	8.94	7.04	6.03	5.71	5.37	5.01	4.19	3.35	2.61	5.8	55.3
16	NB	195+10	8.9	7.4	6.24	5.78	5.38	4.97	4.11	3.26	2.56	6.24	55.7
17	NB	205+12	8.34	7.2	6.91	6.59	6.16	5.63	4.57	3.63	2.8	5.83	54.6
18	NB	215+22	8.51	7.92	7.27	7.09	6.78	6.35	5.38	4.42	3.48	6.99	54.2
19	NB	225+34	8.35	6	5.85	5.8	5.59	5.17	4.28	3.48	2.77	5.41	56
20	NB	235+41	8.46	7.43	6.93	6.67	6.28	5.87	5.01	4.2	3.51	7.64	57.1
21	NB	245+64	8.4	5.53	5.2	5.11	4.91	4.66	4.03	3.38	2.71	4.9	56.4
22	NB	255+59	8.33	6.29	5.69	5.22	4.55	3.94	2.85	2.07	1.61	5.07	54.6
23	NB	268+29	8.03	10.3	10.18	10.13	10.06	9.95	6.59	5.48	4.43	9.29	56.8
24	NB	278+47	8.41	8.3	8.21	8.12	7.94	7.72	6.68	5.4	4.19	7.64	55.7
25	NB	289+31	8.48	6.88	6.32	6.06	5.83	5.58	4.93	4.25	3.52	6.01	56
26	NB	298+06	8.47	6.61	6.56	6.54	6.46	6.39	5.79	4.85	3.97	6.18	54.9
27	NB	308+11	8.53	6.75	6.13	5.9	5.69	5.46	4.87	4.3	3.69	6.04	55.7
28	NB	328+10	8.24	8.4	7.73	7.35	7.01	6.71	6.11	5.43	4.78	7.03	55.3
29	NB	328+17	8.36	7.94	6.99	6.64	6.3	5.98	5.32	4.48	3.73	6.61	55.3
30	NB	338+19	8.48	8.64	7.84	7.44	7.1	6.85	6.17	5.29	4.48	7.27	55.7
31	NB	348+23	8.4	11.05	10.35	10.18	9.93	9.62	8.87	7.95	7.05	10.34	51.6
32	NB	358+32	8.22	8.96	8.12	7.84	7.53	7.19	6.32	5.42	4.47	7.82	55.3
33	NB	368+44	8.3	8.47	7.22	6.78	6.4	6.03	5.25	4.44	3.61	7.11	52.7
34	NB	377+94	8.35	13.32	11.54	10.97	10.45	9.98	8.88	7.72	6.56	11.58	51.6
35	NB	388+04	8.36	9.06	7.64	7.16	6.68	6.22	5.27	4.41	3.63	7.96	56
36	NB	398+59	8.31	7.45	6.55	6.12	5.71	5.37	4.66	3.97	3.32	6.25	56.4
37	NB	408+09	8.25	5.63	5.11	4.96	4.82	4.59	4.03	3.4	2.85	4.85	56
38	NB	417+89	7.89	5.47	5.59	5.26	4.94	4.5	3.59	2.74	2.22	4.46	56.4
38	NB	419+49	8.39	13.51	11.06	9.38	7.65	6.27	4.29	3.1	2.23	9.9	55.7
39	NB	428+02	8.37	7.64	6.96	6.76	6.55	6.3	5.63	4.9	4.24	6.71	56
40	NB	437+08	8.12	12.11	11.23	10.83	10.26	9.69	8.43	7.27	6.19	12.25	56.8
41	NB	447+90	8.34	8.47	7.64	7.22	6.77	6.34	5.44	4.52	3.61	8.25	56
42	NB	459+03	8.11	10.02	9.04	8.7	8.35	7.96	7.06	6.13	5.17	9.2	54.6
43	NB	465+36	8.41	9.43	8.39	7.82	7.31	6.91	6.02	5.1	4.26	8.22	57.9
44	NB	475+02	8.18	6.28	6.1	5.92	5.74	5.54	5	4.4	3.74	5.8	59.7
45	NB	484+11	8	9.2	8.67	8.51	8.2	7.79	6.86	5.76	4.7	8.52	58.2
46	NB	491+10	8.12	7.79	7.34	7.19	6.9	6.55	5.66	4.72	3.81	6.93	58.2
47	NB	500+16	8.39	7.19	6.89	6.74	6.47	6.13	5.31	4.47	3.67	6.69	59.7
48	NB	508+19	8.35	5.15	5.01	4.89	4.67	4.43	3.85	3.26	2.7	4.9	59.7
49	NB	517+42	8.23	8	7	6.33	5.4	4.57	3.18	2.18	1.8	7.06	56.4
50	NB	518+92	8.24	6.03	5.36	4.93	4.35	3.82	2.84	2.09	1.69	4.74	57.9

Table A-2 Southbound Lane Preconstruction FWD Data (Performed on 5/21/2002 on Previous Existing AC Roadway Surface)

TS #	Lane	Station	Load (kip)	Sensor Number / Location									Pav't Temp
				1	2	3	4	5	6	7	8	9	
				d_0	d_8	d_{12}	d_{18}	d_{24}	d_{36}	d_{48}	d_{60}	d_{-12}	
1	SB	525+02	8.18	6.15	5.6	5.17	4.57	4	2.91	2.07	1.66	4.89	58.2
2	SB	508+30	8.39	8.57	7.95	7.68	7.25	6.75	5.73	4.77	3.86	8.48	58.2
3	SB	498+74	8.56	9.34	8.69	8.46	8.05	7.64	6.66	5.65	4.7	8.86	57.9
4	SB	489+67	8.33	8.39	7.92	7.63	7.34	7.03	6.18	5.13	2.55	7.37	57.1
5	SB	480+01	8.04	6.41	5.8	5.61	5.46	5.26	4.73	4.11	3.47	5.34	58.2
6	SB	470+04	8.24	7.3	6.36	5.9	5.41	4.99	4.11	3.28	2.5	6.11	58.6
7	SB	462+84	8.28	8.54	7.45	7.12	6.88	6.58	5.81	5.05	4.27	7.28	58.6
8	SB	450+85	8.01	6.9	6.22	5.8	5.44	5.21	4.71	4.03	3.45	5.61	57.5
9	SB	441+05	8.41	9.51	9.04	8.9	8.62	8.29	7.4	6.46	5.44	8.91	58.6
10	SB	431+08	8.19	7.36	6.84	6.34	5.98	5.71	5.11	4.47	3.78	5.95	60.1
11	SB	420+99	8.45	6.85	6.24	6.04	5.78	5.48	4.73	3.97	3.22	6.22	59.7
12	SB	411+34	8.34	8.13	7.53	7.29	7.01	6.74	6.06	5.29	4.56	7.74	59.7
13	SB	401+13	8.53	6.73	5.91	5.67	5.44	5.16	4.51	3.82	3.22	5.73	58.6
14	SB	391+07	7.96	8.96	8.21	7.8	7.42	7.07	6.2	5.33	4.47	8.71	59.7
15	SB	381+43	8.31	7.84	7.37	7.23	6.99	6.7	5.98	5.19	4.39	7.26	59.7
16	SB	371+00	8.22	8.03	7.07	6.54	5.96	5.49	4.68	3.89	3.15	6.5	59.7
17	SB	360+76	8.14	7.64	7.37	6.78	6.31	5.9	4.92	4.02	3.22	6.34	59.7
18	SB	350+83	8.15	8.62	7.73	7.43	7.08	6.72	5.9	5.05	4.22	7.34	60.1
19	SB	340+67	8.51	8.61	8.18	8	7.74	7.48	6.75	5.91	5.09	8.14	59.7
20	SB	331+00	8.48	7.14	6.63	6.44	6.23	6.01	5.38	4.7	3.99	6.37	59.7
21	SB	321+05	8.09	8.24	7.65	7.53	7.35	7.1	6.38	5.56	4.74	7.43	59.3
22	SB	310+86	8.28	7.54	6.48	6.22	5.93	5.6	4.84	4.08	3.38	6.17	60.8
23	SB	300+87	8.11	9.04	8.75	8.59	8.27	7.91	7.03	5.97	4.57	8.63	59.7
24	SB	291+14	8.31	5.85	5.47	5.29	5.05	4.78	4.18	3.57	3	5.5	53.1
25	SB	279+94	8.01	9.45	8.65	8.26	7.91	7.42	6.37	5.33	4.33	7.78	63
26	SB	270+96	8.06	12.63	10.73	10.04	9.15	8.29	6.62	5.25	4.06	10.86	63
27	SB	260+26	8.03	7.14	6.42	5.89	5.18	4.54	3.38	2.5	2.09	7.01	60.4
28	SB	250+05	8.03	6.5	6	5.84	5.51	5.16	4.37	3.59	2.86	6.04	62.6
29	SB	240+08	8.36	5.63	5.42	5.31	5.1	4.73	3.83	3.05	2.34	5.09	62.6
30	SB	230+05	7.96	6.19	6.15	6.09	5.96	5.73	4.77	3.95	3.26	5.71	51.6
31	SB	219+35	8.14	8.56	8.49	8.49	8.35	7.66	6.14	4.85	3.7	7.2	64.8
32	SB	209+93	8.03	6.2	5.97	5.83	5.57	5.26	4.47	3.68	2.93	5.74	63.7
33	SB	199+95	8.26	7.51	5.8	5.03	4.52	4	3.09	2.39	1.77	4.92	65.2
34	SB	189+83	8.11	5.63	4.81	4.61	4.42	4.18	3.57	2.92	2.33	4.56	64.5
35	SB	175+90	8.11	6.21	6.05	5.94	5.74	5.49	4.93	4.37	2.26	5.88	63.4
36	SB	165+87	8.44	5.64	5.2	5.07	4.87	4.65	4.04	3.4	2.75	5.05	64.5
37	SB	155+59	7.92	3.48	3.28	3.18	3.04	2.92	2.69	2.5	2.37	3.02	64.5
38	SB	144+80	7.92	7.93	7.21	6.74	6.25	5.82	4.88	4.02	3.15	6.68	66.3
39	SB	136+24	8.34	5.61	4.96	4.81	4.64	4.44	3.9	3.36	2.76	4.59	63.4
40	SB	126+07	8	8.02	7.72	7.58	7.26	6.91	6.05	5.2	2.66	7.4	66.3
41	SB	116+26	8.07	6.19	6.05	5.91	5.67	5.35	4.56	3.77	3.03	5.76	67
42	SB	106+06	8.28	6.25	5.54	5.34	5.14	4.92	4.29	3.64	2.97	5.35	67.7
43	SB	95+29	8.11	6.24	6.16	6.01	5.83	5.6	4.95	4.23	3.48	5.6	66.7
44	SB	85+34	8.45	10.16	8.67	8.11	7.41	6.69	5.33	4.14	3.06	8.63	71.4
45	SB	75+41	8.17	6.75	6.1	5.9	5.62	5.3	4.51	3.72	3	6.15	71.8
46	SB	65+97	8.39	4.65	4.13	3.94	3.69	3.42	2.83	2.27	1.76	4.22	69.9
47	SB	55+95	8.4	8.45	7.77	7.29	6.59	5.89	4.55	3.31	2.11	6.97	70.7
48	SB	45+84	7.91	2.56	2.41	2.34	2.26	2.12	1.81	1.5	0	2.14	57.5

APPENDIX B

Table B-1 Soil Classification of Iowa Highway 13

TS #	Stations	Soil Classification									
		USDA Classification					AASHTO	Visual Classification			
		Stations	Soil Name	Sample Depth	USDA Texture	Unified		Stations	Sample Depth / Size	Visual Description	Visual Classification (unified)
9	52 to 56	51 to 63	Waspie Loam	0"-11"	Loam	CL, ML, CL-ML	A-4	54+27			
				11"-29"	Loam, sandy loam, sandy clay	CL, SC, CL-ML, SM-SC			14"-20"	Top 6" dark brown sand with silt	SM
				29"-60"	Gravelly loamy sand, Gravelly sand, sand	SW, SM, SP, SP-SM		14"-40"			
									20"-40"	Brown to yellowish brown fine sand.	SP
									44"-56"	Top 12" brown to yellowish brown fine sand.	SP
								44"-74"	56"-62"	6" gray sandy silty lenses	SP-SM
									62"-74"	Bottom 12" yellowish brown poorly graded sand.	SP
									102"-122"	Yellowish orange to orangish brown well graded sand.	SW
11	57 to 61	51 to 63	Waspie Loam	0"-11"	Loam	CL, ML, CL-ML	A-4	58+24			
				11"-29"	Loam, sandy loam, sandy clay	CL, SC, CL-ML, SM-SC			14"-40"	Brown to yellowish brown fine sand with silt.	SM
									46"-75"	Yellowish orange well graded sand with some larger particles.	SW
				29"-60"	Gravelly loamy sand, Gravelly sand, sand	SW, SM, SP, SP-SM					SW
									144"-166"	Yellowish orange to orange yellow well graded sand with some larger particles.	

15	67 to 71	68 to 72	Lawler Loam				A-6, A-7	68+50			
				0"-17"	Loam	CL, ML			12"-38"	Dark brown fine grained sand with yellowish orange well graded sand lenses with some fine gravel.	SW-SM
				17"-28"	Loam, sandy clay loam, clay loam	CL, SC			72"-97"	Brown to yellowish brown well graded sand	SW
				28"-60	Gravelly coarse sand, gravelly loamy sand, loamy coarse sand	SW, GP, SP, SW-SM			107"-117"	Yellowish brown well graded sand with some larger particles.	SW
								107"-135" Saturated	117"-125"	Yellowish brown clayey sand.	SC
									125"-135"	Yellowish brown fine sand with few larger particles.	SP
21	82 to 86	80 to 84	Clyde - Floyd Complex				Clyde A-7, Floyd A-6, A-7	81+50			
			Clyde	0"-23"	Clay loam	OL, MH, ML, OH			14"-24"	Dark brown sandy silt	CL
				23"-34"	Clay loam, loam, silty clay loam.	CL, ML		14"-36"	24"-26"	Yellowish/brown sandy clay	CL
				34"-41"	Sandy loam, loam, sandy clay loam.	SM, SM-SC			26"-36"	Dark brown sandy silt	SC
				41"-60"	Loam, sandy clay loam.	CL,SC			72"-101"	Yellowish/brown sandy clay with gray mottling	ML-CL
									102"-122"	Dark gray sandy clay, massive with some 1/2" particle	CL
		84 to 92	Floyd	0"-22"	Loam	OL, ML, CL	A-6				
				22"-30"	Sandy clay loam, loam.	CL					

				30"-36"	Sandy loam, loamy sand	SM, SM-SC					
				36"-60"	Loam, clay loam, sandy clay loam.	CL					
23	87 to 91	84 to 92	Kenyon Loam	0"-17"	Loam	CL	A-6	88+50	12"-38"	Yellowish/brown sandy clay with gray mottling at the top	CL
				17"-54"	Loam, clay loam, sandy clay loam.	CL			41"-66"	Yellowish/orange to brown sandy clay	CL
				54"-60"	Loam	CL					
31	107 to 113	101 to 117	Kenyon Loam	0"-17"	Loam	CL	A-6	108+55	48"-73"	Yellowish/orange with gray mottling	CL
				17"-54"	Loam, clay loam, sandy clay loam.	CL			116"-128"	Yellowish/orange with gray mottling	CL
				54"-60"	Loam	CL					
36	125 to 129	121 to 153	Kenyon Loam	0"-17"	Loam	CL	A-6	126+80			
								18"-44"	18"-36"	Yellowish/brown sandy-clay with light gray mottling	CL
				17"-54"	Loam, clay loam, sandy clay loam.	CL			36"-44"	Brown sandy-clay with 1/2" particles	CL
				54"-60"	Loam	CL		56"-67"	56"-63"	Gray-fine sand with clay	CL
									63"-67"	Brownish gray fine sand with silt and organic matter (roots)	CL
								120" Bag sample		Saturated gray sand with clay and yellow clay nodules	CL
73	219 to 223	215 to	Olin Fine				A-2, A-4	219+73			

		220	Sandy Loam	0"-28"	Fine sandy loam, sandy loam.	SM-SC, SC			13"-37"	Yellowish/brown sandy-clay with gray mottling and particle up to one inch	CL
				28"-46"	Loam, clay loam, sandy clay loam.	CL, SC			48"-72"	Yellowish/brown uniform in color sandy-clay	CL
				46'-60	Loam, clay loam	CL			102"-121"	Brownish/gray clayey-sand, "massive", with particle up to one inch	CL
75	224 to 228	220 to 229	Clyde - Floyd Complex				Clyde A-7, Floyd A-6, A-7	226+48	Low elevation potential fill material		
			Clyde	0"-23"	Clay loam	OL, MH, ML, OH			16"-43"	Dark brown fine to medium sand	CL, SC
				23"-34"	Clay loam, loam, silty clay loam.	CL, ML			47"-53"	Brown sandy clay	SC
				34"-41"	Sandy loam, loam, sandy clay loam.	SM, SM-SC		47"-70"	53"-70"	Yellow clayey sandy	SC
				41"-60"	Loam, sandy clay loam.	CL,SC			96"-?	Yellow sandy clay (Pinched tube)	SC
									124"-136"	Top-Yellow clay with some sand. Bottom-Fine yellowish/brown clayey sand with few 2" cobbles (possible parent material)	SC
			Floyd	0"-22"	Loam	OL, ML, CL					
				22"-30"	Sandy clay loam, loam.	CL					
				30"-36"	Sandy loam, loamy sand	SM, SM-SC					

				36"-60"	Loam, clay loam, sandy clay loam.	CL					
79	234 to 238	232 to 262	Clyde - Floyd Complex				Clyde A-7, Floyd A-6, A-7	234+50			
			Clyde						12"-36"	Fine dark brown sand with yellow/orangish clay pockets (nodules). Less than 5% large aggregate approximately one inch.	ML
				0"-23"	Clay loam	OL, MH, ML, OH					
				23"-34"	Clay loam, loam, silty clay loam.	CL, ML			44"-53"	Dark brown medium to fine sand (homogeneous)	SM-SC
				34"-41"	Sandy loam, loam, sandy clay loam.	SM, SM-SC		44"-71"	53"-57"	Medium brown medium to fine sand (homogeneous)	SC
				41"-60"	Loam, sandy clay loam.	CL,SC			57"-71"	Dark brown medium to fine sand (homogeneous)	SC
								96"-122"		Yellow medium to coarse sand	SW
				0"-22"	Loam	OL, ML, CL					
				22"-30"	Sandy clay loam, loam.	CL					
			Floyd	30"-36"	Sandy loam, loamy sand	SM, SM-SC					
				36"-60"	Loam, clay loam, sandy clay loam.	CL					
85	249 to 253	232 to 262	Clyde - Floyd Complex				Clyde A-7, Floyd A-6, A-7	252+81			

			Clyde	0"-23"	Clay loam	OL, MH, ML, OH			12"-39"	Dark grayish/brown fine sand with large clay nodules gray in color	CL
				23"-34"	Clay loam, loam, silty clay loam.	CL, ML			72"-76"	Yellow sandy clay	CL
				34"-41"	Sandy loam, loam, sandy clay loam.	SM, SM-SC		72"-86"	76"-86"	Yellow clay with medium sand and gravel. Some mottling gray in color, possibly calcic	CL,SC
				41"-60"	Loam, sandy clay loam.	CL,SC			102"-113"	Yellow clay and very fine sand, bottom 1"-2" very fine cemented sand (possible bedrock or parent material)	CL.SC
			Floyd	0"-22"	Loam	OL, ML, CL					
				22"-30"	Sandy clay loam, loam.	CL					
				30"-36"	Sandy loam, loamy sand	SM, SM-SC					
				36"-60"	Loam, clay loam, sandy clay loam.	CL					
93	270 to 274	271 to 280	Kenyon Loam	0"-17"	Loam	CL	A-6	275+22	22"-47"	Light brown to yellowish brown, sandy lean clay with particle coatings, minor modeling (yellowish brown with gray patches). Fine gravel to coarse sand increasing with depth of sample.	CL

				17"-54"	Loam, clay loam, sandy clay loam.	CL			67"-89"	Oxidized to unoxidized transition 10" from the top of the sample. Light yellowish brown to dark gray in color, well modeled with gravel up to 1 inch in size. Fractures present in the parent material which indicates coated oxidized flow paths.	CL
				54"-60"	Loam	CL			101"-125"	Dark gray stiff clay (unoidized glacial till) below the water table. "Massive" Particle with a maximum size up to one inch. Very little sand.	CL
98	280 to 284	280 to 283	Clyde - Floyd Complex				Clyde A-7, Floyd A-6, A-7	282+31			
			Clyde	0"-23"	Clay loam	OL, MH, ML, OH			39" Bag sample	Yellowish/brown clean medium poorly graded sand	SP, SC
				23"-34"	Clay loam, loam, silty clay loam.	CL, ML			70"-95"	Yellowish/gray sandy clay with large gravel (2"-3")	CL,SC
				34"-41"	Sandy loam, loam, sandy clay loam.	SM, SM-SC					
				41"-60"	Loam, sandy clay loam.	CL,SC					
		283 to 287	Floyd	0"-22"	Loam	OL, ML, CL	A-6				
				22"-30"	Sandy clay loam, loam.	CL					
				30"-36"	Sandy loam, loamy sand	SM, SM-SC					

				36"-60"	Loam, clay loam, sandy clay loam.	CL					
118	330 to 334	329 to 332	Colo-Ely Complex				Colo A-4, A-6, Ely A-7, A-6	331+48			
			Colo	0"-18"	Silty loam	CL,CL-ML		13"-37"	13"-16"	Medium brown fine sand	CL-ML
				18"-47"	Silty clay loam	CL,CH			16"-22"	Yellow brown to brown very clean sand	CL
				47"-60"	Silty clay loam, clay loam, silt loam	CL,CH			22"-37"	Dark brown sandy-silt to dark brown sandy clay towards the bottom	CL, ML
									66"-91"	Dark brown sandy-silt with lots of organic matter (possible fill material)	OH
			Ely	0"-26"	Silty clay loam	CL, OH, MH			104"-133"	Black/dark gray sandy-silt with lots of organic matter (possible top soil)	OH
				26"-49"	Silty clay loam	CL, ML					
				49"-60"	silt loam, silty clay loam, loam.	CL					
122	340 to 344	341 to 344	Fayette Silt Loam				A-4, A-6	342+90			
				0"-12"	Silt loam.	CL-ML, CL		16"-41"	16"-28"	Yellowish/brown with mottling gray in color, blocky structure	CL,ML
				12"-46"	Silty clay loam, clay loam	CL			28"-41"	Dark brown clayey silt	CL-ML
				46"-60"	Silt loam.	CL			67"-75"	Dark brown clayey silt	CL-ML
								67"-83"	75"-83"	Yellowish/brown with mottling gray in color, blocky structure	CL
									102"-127"	Light gray very fine sandy-silt with iron oxide staining	CL,ML

144	395 to 399	396 to 405	Basset Loam	0"-12"	Loam	CL, CL-ML	A-4, A-6	396+50	12"-26"	Yellowish/brown well graded sand	CL
				20"-42"	Loam, fine sandy loam.	CL		12"-38"	26"-38"	Yellowish/brown sandy-clay with gray mottling	CL-ML
				42"-60"	Loam	CL			42"-71"	Dark gray clay with sand and gravel, "massive"	CL
									96"-124"	Dark gray lean clay with sand.	CL
164	445 to 449	431 to 457	Clyde - Floyd Complex				Clyde A-7, Floyd A-6, A-7	448+50			
			Clyde	0"-23"	Clay loam	OL, MH, ML, OH			10"-31"	Light brown to yellowish/brown sandy-silt, "mottled"	ML
				23"-34"	Clay loam, loam, silty clay loam.	CL, ML			51"-75"	Light gray very fine sandy/silt with iron oxide staining	ML
				34"-41"	Sandy loam, loam, sandy clay loam.	SM, SM-SC			104"-?	Light gray to light brown sandy-silt with orangish sand seams	ML
				41"-60"	Loam, sandy clay loam.	CL,SC					
			Floyd	0"-22"	Loam	OL, ML, CL					
				22"-30"	Sandy clay loam, loam.	CL					
				30"-36"	Sandy loam, loamy sand	SM, SM-SC					
				36"-60"	Loam, clay loam, sandy clay loam.	CL					
166	450 to 454	431 to 457	Clyde - Floyd Complex				Clyde A-7, Floyd A-6, A-7	452+00			

			Clyde	0"-23"	Clay loam	OL, MH, ML, OH		12"-Rock		Yellowish/brown sandy silt with stiff platy structure	ML
				23"-34"	Clay loam, loam, silty clay loam.	CL, ML		96" Bag sample		Yellowish/brown sandy silt with stiff platy structure	ML
				34"-41"	Sandy loam, loam, sandy clay loam.	SM, SM-SC					
				41"-60"	Loam, sandy clay loam.	CL,SC					
			Floyd	0"-22"	Loam	OL, ML, CL					
				22"-30"	Sandy clay loam, loam.	CL					
				30"-36"	Sandy loam, loamy sand	SM, SM-SC					
				36"-60"	Loam, clay loam, sandy clay loam.	CL					
186	495+50 to 499+50	495 to 498	Clyde - Floyd Complex				Clyde A-7, Floyd A-6, A-7	498+00			
			Clyde	0"-23"	Clay loam	OL, MH, ML, OH					
				23"-34"	Clay loam, loam, silty clay loam.	CL, ML		12"-Rock	12"-25"	Yellowish sandy clay with light gray mottling and gravel up to 3/4"	CL
				34"-41"	Sandy loam, loam, sandy clay loam.	SM, SM-SC			25"-27"	Brownish/yellow sandy clay	SC
				41"-60"	Loam, sandy clay loam.	CL,SC		42"-66"	42"-57"	Dark brown fine to coarse sandy clay	CL
		498 to 504	Floyd	0"-22"	Loam	OL, ML, CL	A-6		57"-66"	Dark brown fine sandy clay with 2" seam of yellowish brown fine sand	CL

				22"-30"	Sandy clay loam, loam.	CL			104"-129"	Dark brown fine to coarse sandy clay	CL
				30"-36"	Sandy loam, loamy sand	SM, SM-SC					
				36"-60"	Loam, clay loam, sandy clay loam.	CL					
189	500+50 to 506+50	504 to 507	Clyde - Floyd Complex				Clyde A-7, Floyd A-6, A-7	501+50			
			Clyde	0"-23"	Clay loam	OL, MH, ML, OH			12"-27"	Medium brown fine sand	CL
				23"-34"	Clay loam, loam, silty clay loam.	CL, ML		12"-37"	27"-29"	Yellowish/brown sandy clay	CL
				34"-41"	Sandy loam, loam, sandy clay loam.	SM, SM-SC			29"-37"	Dark brown fine to medium sand with silt and grayish/green clay lenses	CL
				41"-60"	Loam, sandy clay loam.	CL,SC			44"-69"	Dark brown/gray silty clay with organic material (possible fill material)	SC
									99"-101"	Brown medium sandy clay	CL
			Floyd	0"-22"	Loam	OL, ML, CL		99"-122"	101"-110"	light yellowish/brown sandy clay with gray mottling	CL
				22"-30"	Sandy clay loam, loam.	CL			110"-122"	Grayish sandy clay with gravel up to one inch	CL
				30"-36"	Sandy loam, loamy sand	SM, SM-SC					
				36"-60"	Loam, clay loam, sandy clay loam.	CL					
191	507+60	507	Kenyon				A-6	509+60			

	to 513+70	to 510	Loam	0"-17"	Loam	CL		16"-42"	Dark brown medium sand with 2" yellow sand seam 10" from top	CL
				17"-54"	Loam, clay loam, sandy clay loam.	CL		34"-40"	Dark brown clean sand	CL
				54"-60"	Loam	CL		96" Bag sample	Yellow fine to medium sand, "saturated"	CL

APPENDIX C

Table C-1 Iowa Highway 13 – Whitetopping Input Parameters

Iowa Highway 13 - Whitetopping Input Parameters		
Existing Pavement Conditions		
Mean Monthly Air Temperature, ºF		61
Joint Spacing, in		108
Thickness of the Asphalt Layer, in		5
Poisson's Ratio of the Asphalt		0.35
Thickness of the PCC Layer, in		7
Poisson's Ratio of the PCC		0.15
Asphalt Layer's Mix Information		
Percent Aggregate Passing #200 Sieve		6
Asphalt Content, Percent by Weight of Mix		5.5
Percent Air Voids		4
Original pen_{25}		90
Aged pen_{25}		58.5
η_{Aged}		3.92
Design Values		
Concrete Flexural Strength, psi		650
Asphalt Elastic Modulus, psi		1354680
	Bonded Conditions	Unbonded Conditions
Modulus of Subgrade Reaction, pci	150	143
PCC Elastic Modulus at 75% Cumulative, psi	3100000	3700000
Effective Thickness of Existing Pavement, in	10.4	9.69

Table C-2 Backcalculation of Properties for Unbonded AC/PCC Pavement

d_{PCC} (mils)	$AREA_{PCC}$	Radius of Relative Stiffness, l	L/l_{est}	AF d_o	AF l	Adj d_{PCC}	Adj l	k-Value	E_{PCC}
3.91	33.378	61.281	1.762	0.637	0.705	2.657	43.184	225	26735656
8.48	28.319	27.868	3.875	0.869	0.926	7.597	25.819	217	3296409
7.18	31.999	45.702	2.363	0.732	0.813	5.444	37.139	148	9622304
8.22	32.888	54.536	1.980	0.675	0.752	5.729	40.989	116	11159612
12.09	29.032	30.115	3.586	0.851	0.914	10.505	27.511	138	2713016
8.39	32.112	46.656	2.315	0.726	0.806	6.275	37.610	125	8562488
7.39	31.555	42.354	2.550	0.756	0.835	5.781	35.381	153	8214035
7.75	32.794	53.421	2.022	0.682	0.759	5.463	40.565	124	11460076
7.02	33.318	60.349	1.790	0.642	0.711	4.674	42.918	129	15009880
5.38	31.290	40.592	2.661	0.768	0.847	4.335	34.388	216	10342104
8.34	29.769	32.863	3.286	0.828	0.897	7.121	29.477	178	4605059
6.39	31.499	41.966	2.573	0.758	0.838	5.046	35.167	178	9295639
7.40	29.816	33.057	3.267	0.827	0.896	6.333	29.611	199	5226191
8.03	30.926	38.413	2.812	0.785	0.862	6.504	33.096	155	6377404
7.83	28.225	27.598	3.913	0.871	0.928	7.052	25.611	237	3493146
9.11	27.359	25.328	4.264	0.890	0.940	8.345	23.817	231	2544815
8.97	31.726	43.581	2.478	0.747	0.827	6.890	36.045	124	7156130
8.89	33.406	61.711	1.750	0.635	0.702	5.811	43.302	102	12291940
9.33	32.626	51.567	2.094	0.694	0.772	6.653	39.821	105	9064358
6.80	32.508	50.341	2.145	0.701	0.781	4.956	39.302	145	11851528
8.17	28.907	29.696	3.637	0.854	0.916	7.198	27.202	207	3868906
11.49	31.082	39.314	2.747	0.778	0.856	9.140	33.639	107	4690674
13.16	30.010	33.878	3.188	0.820	0.891	11.000	30.174	110	3126131
10.20	30.858	38.030	2.840	0.788	0.864	8.240	32.861	124	4962332
8.39	33.739	67.600	1.598	0.605	0.661	5.232	44.683	107	14544115
10.10	32.349	48.786	2.214	0.711	0.791	7.368	38.612	101	7691383
10.26	30.250	34.956	3.090	0.811	0.884	8.539	30.896	136	4225297
10.56	31.129	39.594	2.728	0.776	0.854	8.394	33.805	116	5159000
9.94	31.352	40.992	2.635	0.765	0.845	7.811	34.618	118	5817474
13.11	32.826	53.803	2.007	0.680	0.757	9.089	40.712	74	6938691
11.49	30.646	36.899	2.927	0.796	0.871	9.357	32.155	114	4181300
10.79	29.274	30.965	3.488	0.844	0.908	9.323	28.131	149	3198973
14.63	28.789	29.309	3.685	0.857	0.918	12.765	26.913	119	2134820
10.81	29.881	33.327	3.241	0.824	0.894	9.129	29.797	136	3672245
10.69	29.808	33.024	3.270	0.827	0.896	9.050	29.588	139	3651421
7.82	30.758	37.485	2.881	0.792	0.868	6.397	32.523	164	6259709
8.75	32.006	45.762	2.360	0.732	0.812	6.596	37.170	122	7954909
13.12	24.897	20.515	5.264	0.930	0.964	12.441	19.771	223	1164727
9.58	31.062	39.199	2.755	0.779	0.856	7.666	33.570	128	5569567
14.09	31.762	43.850	2.463	0.745	0.825	10.689	36.188	79	4650299

Table C-2 (continued)

10.17	29.740	32.744	3.298	0.829	0.898	8.648	29.394	148	3770224
12.41	30.310	35.233	3.065	0.809	0.882	10.254	31.080	112	3561217
10.60	28.549	28.554	3.782	0.863	0.923	9.379	26.344	169	2781849
8.10	32.524	50.495	2.139	0.700	0.780	5.859	39.368	122	10057702
11.52	32.150	46.982	2.299	0.723	0.804	8.522	37.768	91	6359340
10.87	31.831	44.375	2.434	0.741	0.822	8.249	36.463	101	6118782
9.79	31.645	42.991	2.512	0.751	0.831	7.547	35.729	115	6417899
7.06	30.018	33.914	3.185	0.820	0.890	6.003	30.198	202	5738242

Table C-3 Backcalculation of Properties for Bonded AC/PCC Pavement

d_{PCC} (mils)	$AREA_{PCC}$, in	Radius of Relative Stiffness, l	L/l_{est}	AF d_o	AF l	Adj d_{PCC}	Adj l	k-Value	E_{PCC}
4.04	32.507	50.326	2.146	0.701	0.781	2.925	39.295	246	20071262
8.61	27.986	26.930	4.010	0.877	0.932	7.665	25.091	227	3081716
7.30	31.541	42.258	2.556	0.756	0.836	5.624	35.328	158	8418663
8.35	32.474	49.997	2.160	0.704	0.783	5.968	39.152	122	9766170
12.22	28.790	29.311	3.685	0.857	0.918	10.587	26.915	143	2574506
8.52	31.718	43.524	2.481	0.747	0.827	6.463	36.015	132	7616906
7.52	31.118	39.532	2.732	0.776	0.854	5.940	33.768	164	7274491
7.88	32.356	48.852	2.211	0.711	0.791	5.694	38.642	131	9968407
7.15	32.827	53.806	2.007	0.680	0.757	4.948	40.713	136	12746761
5.51	30.700	37.178	2.905	0.794	0.870	4.480	32.331	236	8831146
8.47	29.408	31.457	3.433	0.839	0.906	7.220	28.485	188	4237073
6.52	30.996	38.814	2.783	0.782	0.859	5.201	33.339	192	8094570
7.53	29.410	31.462	3.433	0.839	0.905	6.432	28.489	211	4757002
8.16	30.533	36.321	2.973	0.801	0.875	6.638	31.787	165	5758470
7.96	27.866	26.610	4.059	0.880	0.933	7.118	24.840	250	3250911
9.24	27.062	24.633	4.384	0.896	0.944	8.399	23.253	241	2407331
9.09	31.363	41.059	2.630	0.765	0.844	7.058	34.656	131	6452419
9.02	33.015	56.121	1.924	0.666	0.741	6.097	41.561	106	10783664
9.46	32.265	48.000	2.250	0.717	0.797	6.874	38.250	110	8088858
6.93	32.017	45.852	2.355	0.731	0.812	5.165	37.215	155	10183666
8.30	28.552	28.566	3.781	0.863	0.923	7.277	26.353	218	3587591
11.62	30.804	37.737	2.862	0.790	0.866	9.280	32.680	112	4356824
13.28	29.778	32.899	3.283	0.828	0.897	11.106	29.502	114	2957979
10.33	30.548	36.396	2.967	0.800	0.875	8.371	31.835	130	4580083
8.52	33.321	60.387	1.788	0.642	0.711	5.555	42.929	109	12634151
10.22	32.018	45.862	2.355	0.731	0.812	7.570	37.219	106	6950015
10.39	29.950	33.621	3.212	0.822	0.892	8.651	29.998	142	3928189
10.69	30.826	37.858	2.853	0.789	0.865	8.536	32.755	121	4758940
10.07	31.029	39.002	2.769	0.780	0.858	7.961	33.452	124	5324775
13.24	32.566	50.930	2.121	0.698	0.777	9.326	39.554	76	6379165
11.62	30.374	35.538	3.039	0.807	0.880	9.482	31.280	119	3901748
10.92	29.000	30.008	3.599	0.851	0.914	9.409	27.432	155	3011086
14.76	28.590	28.683	3.765	0.862	0.922	12.843	26.441	122	2046894
10.94	29.601	32.191	3.355	0.834	0.901	9.230	29.006	142	3438589
10.81	29.525	31.899	3.386	0.836	0.903	9.150	28.800	145	3418808
7.95	30.357	35.459	3.046	0.807	0.881	6.524	31.227	174	5651810
8.88	31.630	42.880	2.519	0.752	0.832	6.777	35.669	129	7122640
13.25	24.714	20.228	5.339	0.932	0.965	12.471	19.519	228	1131598
9.71	30.730	37.340	2.892	0.793	0.869	7.805	32.433	135	5101387
14.22	31.529	42.177	2.561	0.757	0.837	10.859	35.283	82	4348601

Table C-3 (continued)

10.30	29.443	31.588	3.419	0.838	0.905	8.746	28.579	154	3520957
12.54	30.061	34.098	3.167	0.818	0.889	10.368	30.323	116	3350116
10.73	28.279	27.751	3.892	0.870	0.927	9.451	25.729	176	2630748
8.23	32.109	46.630	2.316	0.726	0.806	6.071	37.597	129	8844517
11.65	31.862	44.609	2.421	0.740	0.820	8.713	36.584	95	5832006
11.00	31.529	42.177	2.561	0.757	0.837	8.422	35.284	106	5607258
9.92	31.313	40.738	2.651	0.767	0.846	7.711	34.473	121	5842552
7.19	29.589	32.146	3.360	0.834	0.901	6.107	28.975	215	5185685

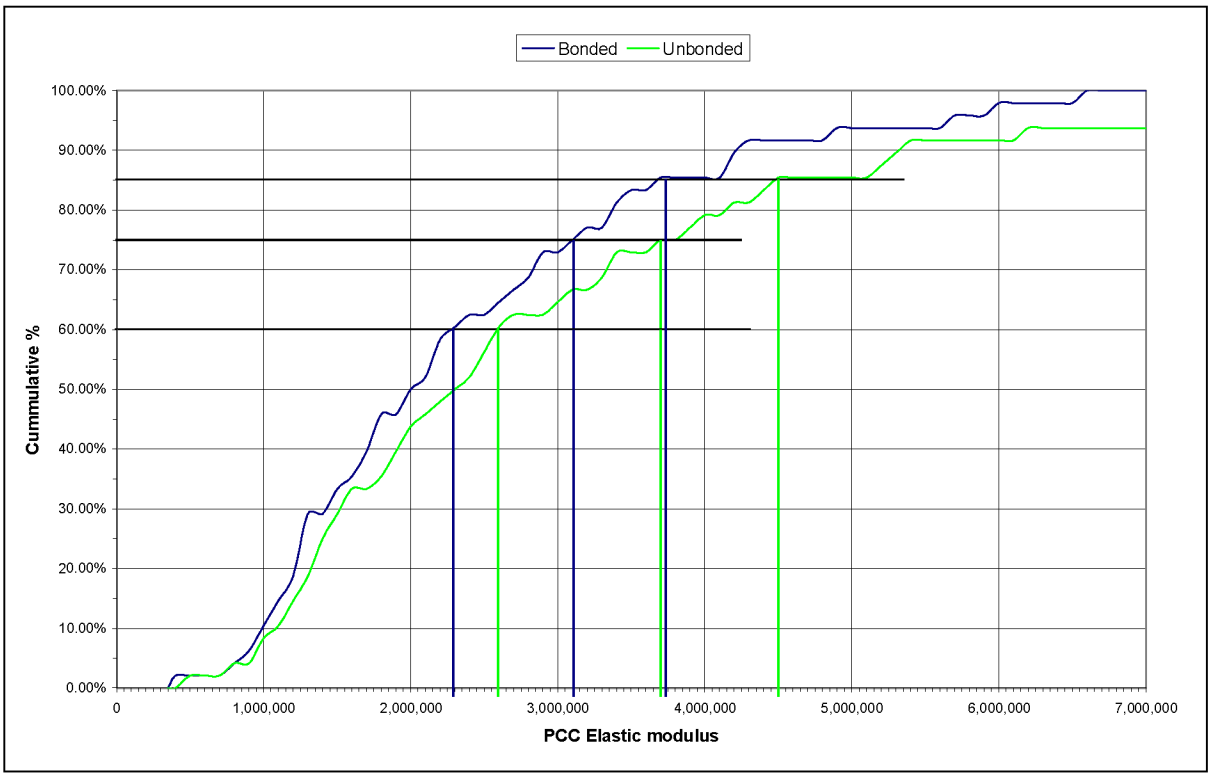

Figure C-1 Cumulative Percentage Plot of the PCC Elastic Modulus

APPENDIX D

Westergaard's Calculation for the "Equivalent" Plate of an Unbonded AC/PCC Pavement in which, "1" indicates the AC properties and "2" indicates the PCC properties.

$P := 9000$

$\mu := .35$

$k := 151$

$a := 6.77$

$fc := 4500$

$E1 := 1354679$

$E2 := 3100000$

$E := E1 \rightarrow 1354679$

$h1 := 5$

$h2 := 7.0$

Two Layers - Unbonded Condition

$$he := \left[\left(\frac{E1}{E}\right)\cdot h1^3 + \left(\frac{E2}{E}\right)\cdot h2^3\right]^{\frac{1}{3}} \qquad he = 9.69$$

$$L := \left[\frac{\left(E\cdot he^3\right)}{\left[12\left(1-\mu^2\right)\cdot k\right]}\right]^{.25} \qquad L = 29.673$$

Interior Loading - Unbonded

$$b := \sqrt{\left(1.6\cdot a^2 + he^2\right)} - 0.675\cdot he \qquad b = 6.391$$

$$\sigma e := \frac{\left[3\cdot\left(1+\mu\right)\cdot P\right]}{\left[3.14159\cdot(2)\cdot he^2\right]}\cdot\left[\ln\left[\frac{(L)}{b}\right] + 0.6159\right] \qquad \sigma e = 132.905$$

$$\Delta e := \left(\frac{P}{8\cdot k\cdot L^2}\right)\cdot\left[1 + \left(\frac{1}{2\cdot 3.14159}\right)\cdot\left(\ln\left(\frac{a}{2\cdot L}\right) - 0.673\right)\cdot\left(\frac{a}{L}\right)^2\right] \qquad \Delta e = 0.00826$$

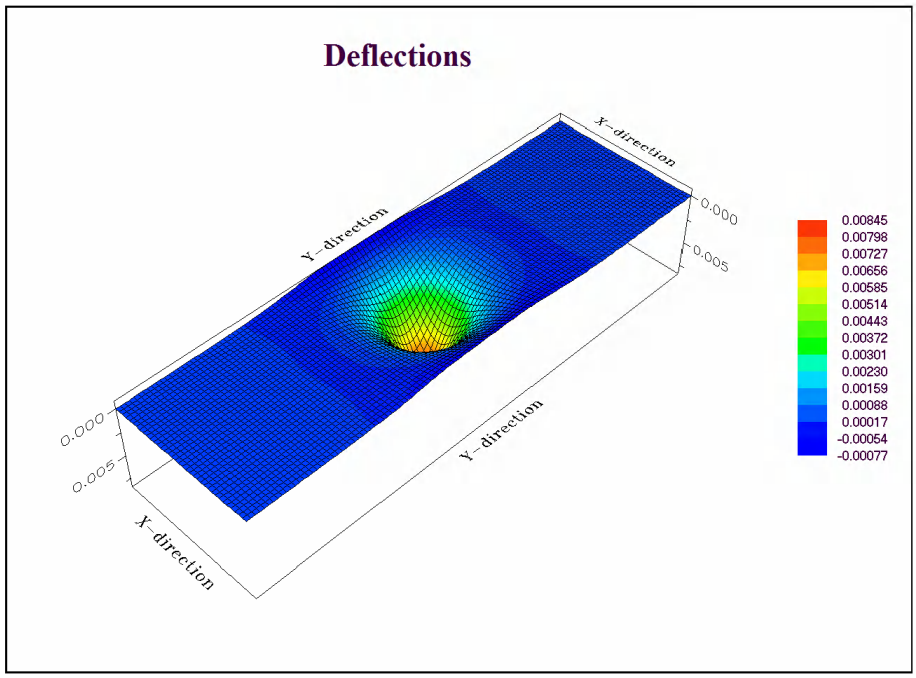

Figure X-X Deflected Shape, "equivalent" Slab Thickness, he=9.6 inches, CL = 62.5 psi, ISLAB2000 Graphical Output

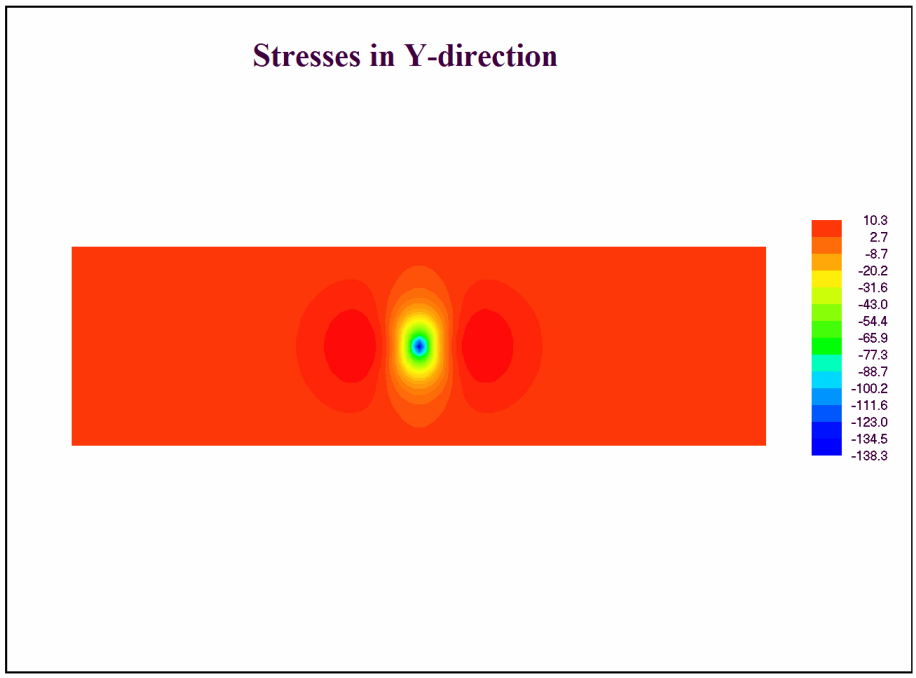

Figure X-X Longitudinal Stress, Top of "equivalent" Slab, he=9.6 inches, CL = 62.5 psi, ISLAB2000 Graphical Output

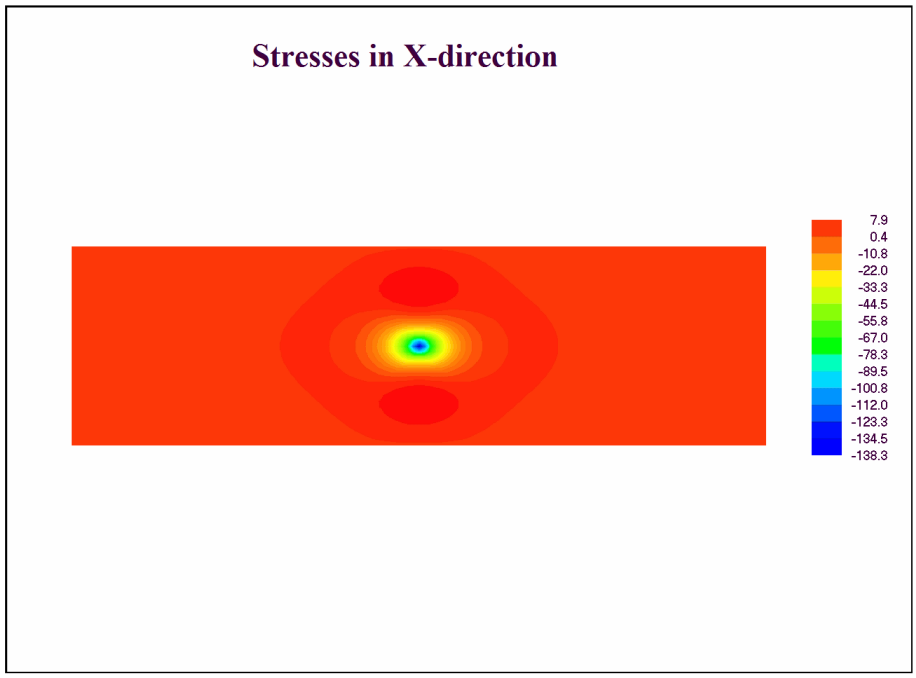

Figure X-X Transverse Stress, Top of "equivalent" Slab, he=9.6 inches, CL = 62.5 psi, ISLAB2000 Graphical Output

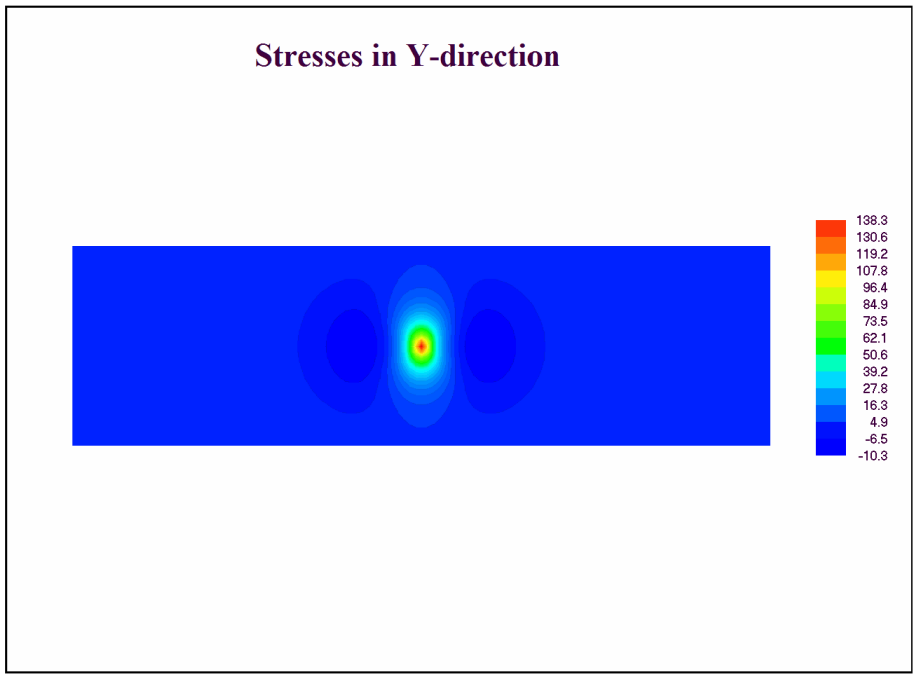

Figure X-X Longitudinal Stress, Bottom of "equivalent" Slab Thickness, he=9.6 inches, CL = 62.5 psi, ISLAB2000 Graphical Output

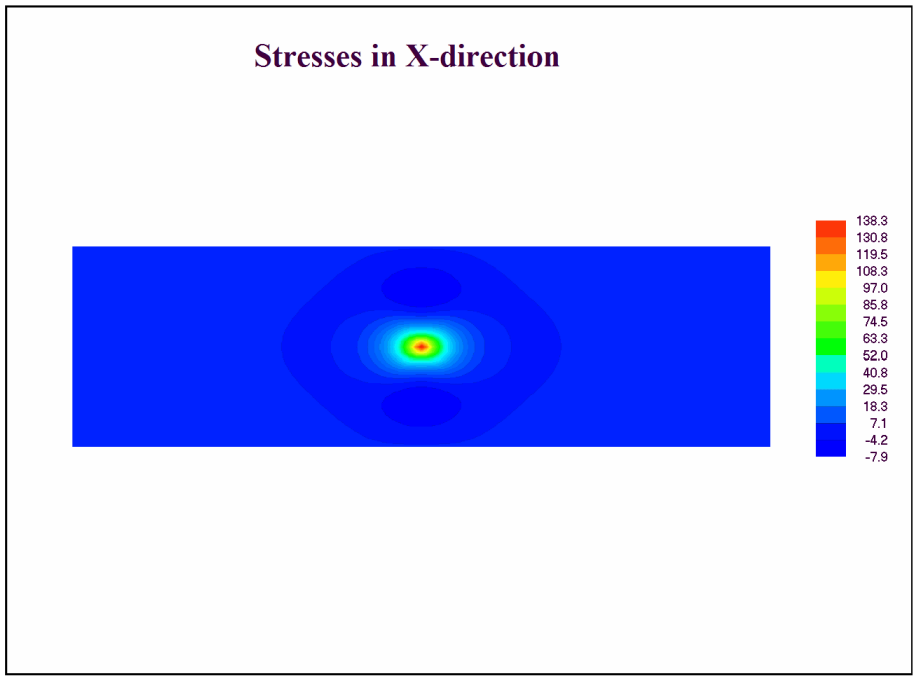

Figure X-X Transverse Stress, Bottom of "equivalent" Slab Thickness, CL = 62.5 psi, ISLAB2000 Graphical Output

APPENDIX E

Westergaard's Calculation for the "Equivalent" Plate of an Unbonded AC/PCC Pavement in which, "1" indicates the AC properties and "2" indicates the PCC properties.

$P := 9000$

$\mu := .35$

$k := 151$

$a := 6.77$

$fc := 4500$

$E1 := 1354680$

$E2 := 3100000$

$E := E1 \rightarrow 1354680$

$h1 := 5$

$h2 := 7.0$

Two Layered - Unbonded Condition

$$he := \left[\left(\frac{E1}{E}\right)\cdot h1^3 + \left(\frac{E2}{E}\right)\cdot h2^3\right]^{\frac{1}{3}}$$

$$he = 9.69$$

$$L := \left[\frac{\left(E\cdot he^3\right)}{\left[12\left(1-\mu^2\right)\cdot k\right]}\right]^{.25}$$

$$L = 29.673$$

Interior Loading - Unbonded

$$b := \sqrt{\left(1.6\cdot a^2 + he^2\right)} - 0.675\cdot he$$

$$b = 6.391$$

$$\sigma e := \frac{\left[3\cdot\left(1+\mu\right)\cdot P\right]}{\left[3.14159\cdot(2)\cdot he^2\right]}\cdot\left[\ln\left[\frac{(L)}{b}\right] + 0.6159\right]$$

$$\sigma e = 132.905$$

$$\Delta e := \left(\frac{P}{8\cdot k\cdot L^2}\right)\cdot\left[1 + \left(\frac{1}{2\cdot 3.14159}\right)\cdot\left(\ln\left(\frac{a}{2\cdot L}\right) - 0.673\right)\cdot\left(\frac{a}{L}\right)^2\right]$$

$$\Delta e = 0.00826$$

Stresses in the bottom of each layer (Ioannides)

$$\sigma 1 := \left(\frac{h1}{he}\right)\cdot \sigma e$$

$$\sigma 1 = 68.577$$

$$\sigma 2 := \left(\frac{h2}{h1}\right)\cdot\left(\frac{E2}{E1}\right)\sigma 1$$

$$\sigma 2 = 219.701$$

Westergaard's Calculation for the "Equivalent" Plate of a Bonded AC/PCC Pavement in which, "2" indicates the AC properties and "1" indicates the PCC properties.

Bonded Condition

$E2 := 1354680$

$E1 := 3100000$

$E := E1 \rightarrow 3100000$

$h2 := 5$

$h1 := 7.0$

$$x := \frac{E1 \cdot h1 \cdot \left(\frac{h1}{2}\right) + E2 \cdot h2 \cdot \left(h1 + \frac{h2}{2}\right)}{E1 \cdot h1 + E2 \cdot h2}$$

$$x = 4.927$$

$$he := \left[\frac{12}{E}\left[E1 \cdot h1 \cdot \left(x - \frac{h1}{2}\right)^2 + \left(\frac{E1 \cdot h1^3}{12}\right) + E2 \cdot h2 \cdot \left(h1 - x + \frac{h2}{2}\right)^2 + \frac{E2 \cdot h2^3}{12}\right]\right]^{\frac{1}{3}}$$

$$he = 10.376$$

$$L := \left[\frac{\left(E \cdot he^3\right)}{\left[12\left(1 - \mu^2\right) \cdot k\right]}\right]^{.25}$$

$$L = 38.415$$

Interior Loading Bonded

$$b := \sqrt{\left(1.6 \cdot a^2 + he^2\right)} - 0.675 \cdot he$$

$$b = 6.45$$

$$\sigma e := \frac{\left[3 \cdot \left(1 + \mu\right) \cdot P\right]}{\left[3.14159 \cdot (2) \cdot he^2\right]} \cdot \left[\ln\left[\frac{(L)}{b}\right] + 0.6159\right]$$

$$\sigma e = 129.347$$

$$\Delta e := \left(\frac{P}{8 \cdot k \cdot L^2}\right) \cdot \left[1 + \left(\frac{1}{2 \cdot 3.14159}\right) \cdot \left(\ln\left(\frac{a}{2 \cdot L}\right) - 0.673\right) \cdot \left(\frac{a}{L}\right)^2\right]$$

$$\Delta e = 0.00497$$

Stresses in the bottom of each layer (Ioannides)

$$y := h1 - x$$

$$y = 2.073$$

$$\sigma 1top := \frac{2 \cdot (h1 - x)}{he} \cdot \sigma e$$

$$\sigma 1top = 51.678$$

$$\sigma 1bottom := \left(\frac{x}{h1 - x}\right) \cdot \sigma 1top$$

$$\sigma 1bottom = 122.852$$

$$\sigma 2top := \sigma 1top \cdot \left(\frac{E2}{E}\right) \cdot \frac{(h2 + h1 - x)}{x}$$

$$\sigma 2top = 32.416$$

$$\sigma 2bottom := \sigma 1top \cdot \frac{E2}{E}$$

$$\sigma 2bottom = 22.583$$

APPENDIX F

Closed form Calculations for the "Equivalent" Plate and Stress distribution of an Unbonded and Bonded PCC Overlay/AC/PCC Pavement in which, "1" indicates the PCC Overlay properties, "2" indicates the AC properties and "3" indicates existing PCC properties.

$P := 9000$

$\mu := .15$

$k := 150$

$a := 6$

$fc := 4500$

$E1 := 3823680$

$E2 := 1354679$

$E3 := 3100000$

$E := E1 \rightarrow 3823680$

$h1 := 3.5$

$h2 := 5$

$h3 := 7$

Interior Loading - Unbonded

$$he := \left[\left(\frac{E1}{E} \right) \cdot h1^3 + \left(\frac{E2}{E} \right) \cdot h2^3 + \left(\frac{E3}{E} \right) \cdot h3^3 \right]^{\frac{1}{3}}$$

$$he = 7.148$$

$$L := \left[\frac{\left(E \cdot he^3 \right)}{\left[12\left(1 - \mu \right) \cdot k \right]} \right]^{.25}$$

$$L = 30.91$$

$$b := \sqrt{\left(1.6 \cdot a^2 + he^2 \right)} - 0.675 \cdot he$$

$$b = 5.601$$

$$\sigma e := \frac{\left[3 \cdot \left(1 + \mu \right) \cdot P \right]}{\left[3.14159 \cdot (2) \cdot he^2 \right]} \cdot \left[\ln\left[\frac{(L)}{b} \right] + 0.6159 \right]$$

$$\sigma e = 224.772$$

$$\Delta e := \left(\frac{P}{8 \cdot k \cdot L^2} \right) \cdot \left[1 + \left(\frac{1}{2 \cdot 3.14159} \right) \cdot \left(\ln\left(\frac{a}{2 \cdot L} \right) - 0.673 \right) \cdot \left(\frac{a}{L} \right)^2 \right]$$

$$\Delta e = 0.00771$$

Stresses in the bottom of each layer (Ioannides)

$$\sigma 1 := \frac{h1}{he} \cdot \sigma e$$

$$\sigma 1 = 110.057$$

$$\sigma 2 := \frac{h2}{h1} \cdot \left(\frac{E2}{E1}\right) \cdot \sigma 1$$

$$\sigma 2 = 55.702$$

$$\sigma 3 := \frac{h3}{h1} \cdot \left(\frac{E3}{E1}\right) \cdot \sigma 1$$

$$\sigma 3 = 178.454$$

Interior Loading - Bonded

$E1 := 3823680$
$E2 := 1354679$
$E3 := 3100000$
$E := E2 \rightarrow 1354679$
$h1 := 3.5$
$h2 := 5$
$h3 := 7$

$$x := \frac{E1 \cdot h1 \cdot \left(\frac{h1}{2}\right) + E2 \cdot h2 \cdot \left(h1 + \frac{h2}{2}\right) + E3 \cdot h3 \cdot \left[h1 + h2 + \left(\frac{h3}{2}\right)\right]}{E1 \cdot h1 + E2 \cdot h2 + E3 \cdot h3}$$

$$x = 7.752$$

$$he := \left[\frac{12}{E} \cdot \left[\left[x - \left(\frac{h1}{2}\right)\right]^2 \cdot E1 \cdot h1 + \frac{\left(E1 \cdot h1^3\right)}{12} + \frac{\left(E2 \cdot h2^3\right)}{12} + E2 \cdot h2 \cdot \left[h1 - x + \left(\frac{h2}{2}\right)\right]^2 + \frac{\left(E3 \cdot h3^3\right)}{12} + E3 \cdot h3 \cdot \left[h1 + h2 - x + \left(\frac{h3}{2}\right)\right]^2\right]\right]^{\frac{1}{3}}$$

$$he = 20.766$$

$$L := \left[\frac{\left(E \cdot he^3\right)}{\left[12\left(1-\mu^2\right)\cdot k\right]} \right]^{.25}$$

$$L = 51.241$$

$$b := \sqrt{\left(1.6\cdot a^2 + he^2\right)} - 0.675\cdot he$$

$$b = 8.092$$

$$\sigma e := \frac{\left[3\cdot\left(1+\mu\right)\cdot P\right]}{\left[3.14159\cdot(2)\cdot he^2\right]}\cdot\left(\ln\left(\frac{L}{b}\right)+0.6159\right)$$

$$\sigma e = 28.21$$

$$\Delta e := \left(\frac{P}{8\cdot k\cdot L^2}\right)\cdot\left[1+\left(\frac{1}{2\cdot 3.14159}\right)\cdot\left(\ln\left(\frac{a}{2\cdot L}\right)-0.673\right)\cdot\left(\frac{a}{L}\right)^2\right]$$

$$\Delta e = 0.00283$$

Stresses in the each layer (Ioannides)

$$y := h1 + h2 - x$$

$$y = 0.748$$

$$\sigma 2bottom := \left[\frac{2\cdot(h1+h2-x)}{he}\right]\cdot\sigma e$$

$$\sigma 2bottom = 2.033$$

$$\sigma 2top := \left(\frac{x-h1}{h1+h2-x}\right)\cdot\sigma 2bottom$$

$$\sigma 2top = 11.552$$

$$\sigma 1top := \frac{x}{h2-y}\cdot\left(\frac{E1}{E}\right)\cdot\sigma 2top$$

$$\sigma 1top = 59.447$$

$$\sigma 1bottom := \left(\frac{E1}{E}\right)\cdot\sigma 2top$$

$$\sigma 1bottom = 32.606$$

$$\sigma 3top := \left(\frac{E3}{E}\right)\cdot \sigma 2bottom$$

$$\sigma 3top = 4.652$$

$$\sigma 3bottom := \left(\frac{h3 + y}{y}\right)\left(\frac{E3}{E}\right)\cdot \sigma 2bottom$$

$$\sigma 3bottom = 48.173$$

REFERENCES

1. Cable, J.K., M.L. Anthony, F.S. Fanous, and B.M. Phares, *Evaluation of Composite Pavement Unbonded Overlays: Phase I and Phase II*, Iowa DOT Project HR-1093, Center for Portland Cement Concrete Pavement Technology, Iowa State University, Ames, IA, 2003

2. Cable, J.K., H. Ceylan, F.S. Fanous, D. Wood, D. Frentress, T.R. Tabbert, S.Y. Oh, and K. Gopalakrishnan, *Design and Construction Procedures for Concrete Overlay and Widening of Existing Pavements*, IHRB Project TR-511, Center for Portland Cement Concrete Pavement Technology, Iowa State University, Ames, IA, September 2005

3. Cable, J.K., J.M. Hart, and T.J. Ciha, *Thin Bonded Overlay Evaluation*, Iowa DOT Project HR-559, Center for Portland Cement Concrete Pavement Technology, Iowa State University, Ames, IA, 1999

4. Hall, K.T., and Darter, M.I., "Improved Methods for Asphalt-Overlaid Concrete Pavement Backcalculation and Evaluation," *Nondestructive Testing of Pavements and Backcalculation of Moduli (Second Volume) STP 1198*, Harold L. Quintus, Albert J. Bush, III, and Gilbert Y. Baladi, Eds., American Society for Testing and Materials, Philadelphia, 1994

5. Ioannides, A.M., L. Khazanovich and J.L. Becque, "Structural Evaluation of Base Layers in Concrete Pavement Systems," *Transportation Research Record No.1370*, Transportation Research Board, National Research Council, Washington, D.C., 1992

6. *NCHRP Synthesis of Highway Practice 338: Thin and Ultra-Thin Whitetopping,* Transportation Research Board, National Research Council, Washington, D.C., 2004

7. Mack, J.W., L.W. Cole, and J.P. Mohsen, "Analytical Consideration for Thin Concrete Overlays on Asphalt," *Transportation Research Record 1388*, Transportation Research Board, National Research Council, Washington, D.C., 1993

8. Rasmussen, R.O., et al., *Performance and Design of Whitetopping Overlays on Heavily Loaded Pavements*, Final Report for Concrete Pavement Technology Program Task 3(99), 5 vols., Federal Highway Administration, Washington, D.C., July 2003

9. Wu, C.L., S.M. Tarr, R.M. Refai, M.A. Nagi, and M.J. Sheehan, *Development of Ultra-Thin Whitetopping Design Procedure*, PCA Research and Development Serial No. 2124, Portland Cement Association, Skokie, Illinois, 1998

10. Sheehan, M.J., S.M. Tarr, and S. Tayabji, *Instrumentation and Field Testing of Thin Whitetopping Pavement in Colorado and Revision of the Existing Colorado Thin Whitetopping Procedure*, Report No. CDOT-DTD-2004-12, Colorado Department of Transportation, Denver, Colorado, August 2004

11. The Transtec Group, http://www.whitetopping.com/design.asp, 2005

12. Riley, R.C., L. Titus-Glover, J. Mallela, S. Waalkes, and M. Darter. "Incorporation of Probabilistic Concepts into Fatigue Analysis of Ultrathin Whitetopping as Developed for the American Concrete Pavement Association," *Proceedings of the International Conference on Best Practices for Ultrathin and Thin Whitetoppings*, Denver, Colorado, 2005

13. McDaniel, Lisa L., "Using Deflection Basins to Estimate Alternative Joint Reinforcement Load Transfer," *Masters Thesis*, Iowa State University, 1998

14. D.M. Burmister, *The Theory of Stresses and Displacements in Layered Systems and Applications to the Design of Airport Runways*, Proc. HRB, Vol. 23, 1943

15. N. Odemark, *Investigations as to the Elastic Properties of Soils and Design of Pavements According to the Theory of Elasticity*, M.A. Hibbs and J. Silfwerbrand (A. M. Ioannides, ed.), 1990

16. S.P. Timoshenko and S. Woinowsky-Krieger, *Theory of Plates and Shells* 2nd ed., McGraw-Hill, New York, 1973

17. Logan, D.L., *A First Course in the Finite Element Method*, Brooks/Cole, Pacific Grove, California, 2002

18. Huang, Y.H., *Pavement Analysis and Design* 2nd ed., Pearson Education, Inc., Upper Saddle River, NJ, 2004

19. ANSYS User's Manual, ANSYS v.6.1, ANSYS Inc., Canonsburg, PA, 2004

20. Cable, J.K., J.L. Morud, and T.R. Tabbert, *Evaluation of Composite Pavement Unbonded Overlays: Phase III*, IHRB Project TR-478, Center for Portland Cement Concrete Pavement Technology, Iowa State University, Ames, IA, August 2006

21. *Soil Survey of Delaware County, Iowa*, U. S. Department of Agriculture, Washington, D.C., 1986

22. "Thickness Design-Asphalt Pavements for Highway and Streets," *Manual Series No. 1*, The Asphalt Institute, Lexington, KY, 1981

23. Miller, J.S., Uzan, J., and Witczak, M.W., "Modifications of the Asphalt Institute Bituminous Mix Modulus Predictive Equation," *Transportation Research Record No.911*, Transportation Research Board, National Research Council, Washington, D.C., 1983

24. Hall, K.T., "Performance, Evaluation, and Rehabilitation of Asphalt-Overlaid Concrete Pavements," *Ph. D Thesis*, University of Illinois at Urbana-Champaign, 1991

25. Crovetti, J.A. and Tirado-Crovetti, M.R., "Evaluation of Support Conditions Under Concrete Slabs," *Nondestructive Testing of Pavements and Backcalculation of Moduli (Second Volume) STP 1198*, Harold L. Quintus, Albert J. Bush, III, and Gilbert Y. Baladi, Eds., American Society for Testing and Materials, Philadelphia, 1994

26. Bowles, J.E., *Foundation Analysis and Design* 5th ed., McGraw-Hill, New York, 1996

27. Westergaard, H.M., "Stresses in Concrete Runways of Airports," *Proceedings*, Highway Research Board, Volume 19, 1939